C4–C5 fused pyrazol-3-amines: when the degree of unsaturation and electronic characteristics of the fused ring controls regioselectivity in Ullmann and acylation reactions†

Elisabeth Bou-Petit,[a] Arnau Plans,[a] Nieves Rodríguez-Picazo,[a] Antoni Torres-Coll,[a] Cristina Puigjaner,[b] , Mercè Font-Bardia,[b] Jordi Teixidó, [a] Santiago Ramon y Cajal,[c] Roger Estrada-Tejedor[a] and José I. Borrell [*a]

[a] Grup de Química Farmacèutica, IQS School of Engineering, Universitat Ramon Llull, Via Augusta, 390, E-08017 Barcelona, Spain. E-mail: jose.borrell@iqs.url.edu

[b] Unitat de Difracció de Raigs X, Centres Cientificotècnics, Universitat de Barcelona, Lluís Solè i Sabarís 1–3, 08028 Barcelona, Spain

[c] Departamento de Patología, Hospital Universitario Valle de Hebrón, Universidad Autónoma de Barcelona, Passeig Vall d'Hebron 119–129, 08035 Barcelona, Spain

Pyrazol-3-amine is a scaffold present in a large number of compounds with a wide range of biological activities and, in many cases, the heterocycle is C4–C5 fused to a second ring. Among the different reactions used for the decoration of the pyrazole ring, Ullmann and acylation have been widely applied. However, there is some confusion in the literature regarding the regioselectivity of such reactions (substitution at N1 or N2 of the pyrazole ring) and no predictive rule has been so far established. As a part of our work on 3-amino-pyrazolo[3,4-b]pyridones 13, we have studied the regioselectivity of such reactions in different C4–C5 fused pyrazol-3-amines. As a rule of thumb, the Ullmann and acylation reactions take place, predominantly, at the NH and non-protonated nitrogen atom of the pyrazole ring respectively, of the most stable initial tautomer (1H- or 2H-pyrazole), which can be easily predicted by using DFT calculations.

.

INTRODUCTION

The pyrazol-3-amine scaffold (1) is present in more than 124 000 heterocylic compounds covered in the literature with biological activities including antitumoral (2, Linifanib),1 antiinflammatory (3),2 anti-diabetic (4),3 and anti-infective agents (5, Sulfaphenazole)4 (Fig. 1).

The parent unsubstituted heterocycle 6 (R1 = R4 = R5 = H) can present three tautomeric forms (Fig. 2): 1H-pyrazol-3-amine (1H-6), 2H-pyrazol-3-amine (2H-6, also named 1Hpyrazol-5-amine), and the imino form (imino-6). There has been great controversy about which is the most stable tautomer and some initial studies pointed to the lower stability of the imino tautomer imino-6,5 with respect to the amino forms. Moreover, more recent theoretical studies seem to indicate a higher thermodynamic stability of the 1H-pyrazol-3-amine form (1H-6) by 1.6 kcal mol−1 with respect to 2H-pyrazol-3-amine (2H-6) tautomer.6,7

As regards the C4–C5 fused forms of the pyrazol-3-amine scaffold, some of the most widely used include: 4,5,6,7-tetrahydro-1H-indazol-3-amines (1H-7, around 2200 substances), 1Hindazol-3-amines (1H-8, circa 65 000 compounds), and 1H-pyrazolo[3,4-b]pyridin-3-amines (1H-9, more than 9600 structures) and their corresponding 2H-tautomers (Scheme 1).

As a part of our ongoing research in the area of tyrosine kinase inhibitors,8 we synthesized a series of 3-amino-2,4,5,7-tetrahydro-6H-pyrazolo[3,4-b]pyridin-6-ones (13) which include a C4–C5 fused pyrazol-3-amine structure. Thus, among others, we obtained 2H-13a (R = Me) and 2H-13b (R = Ph) upon treatment of the corresponding 2-methoxy-6-oxo-1,4,5,6 tetrahydropyridin-3-carbonitriles 12a–b, obtained from the treatment of α,β-unsaturated esters 10a–b with malononitrile (11) in NaOMe/MeOH, with hydrazine hydrate in MeOH under microwave irradiation at 140 °C (Scheme 1).9 Contrary to the pyrazol-3-amine 6, compounds 13 are depicted as the 2H-tautomer for reasons discussed later in this paper.

Once obtained, we decided to derivatize compounds 2H-13 using two of the reactions most widely used on systems containing the pyrazol-3-amine substructure: the Ullmann and acylation protocols. Then, we realized that there is uncertainty in the literature regarding the nitrogen atom of the pyrazol-3-amine ring at which the derivatization takes place.

Thus, in the case of the pyrazol-3-amine 1H-6, while all the references available indicate that the Ullmann reaction takes place mainly at N1 with yields higher than 80%,10,11 the acylation seems to take place at N1 or at N2.12,13 The situation is even more complex in the case of the fused rings 7–9. There are examples of acylation at N1 or N2 of 1H-7,14 but only at N1 of 1H-815 and 1H-9.16 In some cases, the acylation also takes place at the C3-NH2 group.17 As regards the Ullmann reaction, there are only some examples at N1 of 1H-8.11,18

The lack, to the best of our knowledge, of any theoretical rationalization to justify or predict such behaviour and our own results during the exploration of the Ullmann and acylation reactions on systems 2H-13, included in this paper, led us to carry out an experimental and theoretical study to understand the

85 reactivity of these scaffolds and the importance of the degree of unsaturation and electronic characteristics
86 of the C4–C5 fused rings.
87 The reaction conditions used for the Ullmann and acylation reactions during such experimental
88 study carried out on tautomeric C4–C5 fused pyrazol-3-amines are included in Scheme 2.
89

RESULTS AND DISCUSSION

In a previous paper8 we showed that the treatment of pyridines 12a (R = Me) and 12b (R = Ph) in MeOH at 140 °C under microwave irradiation with phenylhydrazine only affords the N2-phenyl substituted pyrazolo[3,4-b]pyridin-6-ones 2Ph-14a–b (Fig. 3).

With the aim of synthesizing the corresponding N1-phenyl substituted isomer 1Ph-14b (R = Ph), we treated 2H-13b under the Ullmann reaction conditions described by Beyer et al.10 The reaction afforded a single compound, both in the crude material and after isolation in 31% yield, which corresponds again to the N2-phenyl substituted isomer 2Ph-14b (R = Ph), as established by comparison with a sample of 2Ph-14b obtained by cyclization of 12b with phenylhydrazine.8 This result, contrary to expectations according to bibliographic references, led us to perform a calculation19 of the energy values of the 1Hand 2H-tautomers of 13b and the N1-phenyl and N2-phenyl substituted isomers 1Ph-14b and 2Ph-14b, respectively. The energy values obtained for the 1H- and 2H-tautomers of 13b and for the N1- and N2-phenyl substituted pyrazolopyridones 1Ph-14b and 2Ph-14b, clearly indicate that the 2H-tautomer 2H-13b and the N2-phenyl substituted isomer 2Ph-14b are more stable than the corresponding N1 isomers by 2.1 and 1.6 kcal mol−1, respectively. The stability difference between isomers, both in the case of the starting material and the arylated product, will certainly not favour the formation of the N1-arylated isomer. Such a result is also compatible with the observation of a single group of signals in the 1H-NMR spectrum of the unsubstituted starting pyrazolopyridone, regardless of the solvent used, which should consequently correspond to the 2H-tautomer 2H-13b.

To understand the effect of the unsaturation of the C4–C5 fused ring, we introduced a double bond at C4–C5 of the pyrazolo[3,4-b]pyridin-6-one 13b. The 1H-NMR spectrum in d6-DMSO presented the signals of a single compound that was not possible to be unequivocally identified as the 2H-tautomer 2H-15b or the 1H-tautomer 1H-15b (Fig. 3). In this case, the difference of the DFT calculated energies was only of 0.2 kcal mol−1 in favour of the 1H-tautomer 1H-15b.

This compound was treated under the same Ullmann reaction conditions used with 2H-13b. The analysis of the reaction crude showed a complete conversion of the starting material into two different compounds in unequal proportions.

The major product (80%) could be isolated by selective precipitation in water and corresponds to the N2-phenyl substituted isomer 2Ph-16b (Fig. 3). Identification of the product was carried out by direct comparison with a sample obtained by oxidation of 2Ph-14b with DDQ.

Purification of the crude material by column chromatography allowed the isolation of the minor product (~20% by NMR integration). This compound presented the same signal profile as 2Ph-16b but with different chemical shifts. Confirmation of the structure of 1Ph-16b, was done by single crystal X-ray diffraction. The ORTEP diagram and atomic numbering are given in Fig. 4.

Although the predicted energies for 2Ph-16b and 1Ph-16b seemed to indicate that 1Ph-16b would be 0.5 kcal mol−1 more stable than 2Ph-16b, once more the N2-phenyl substituted isomer 2Ph-16b

predominated. The very similar energy between the tautomers is consistent with the formation of both products. In this case, the proportion between the two isomers cannot be explained by such a small energy difference and therefore other factors such as the relative stability of the Cu-complexes can play a determining role. Energy optimization and frequency calculations at B3LYP/def2TZVP level of theory were performed for Cu complexes that lead to 1Ph-16 and 2Ph-16 compounds. Computational study evinces that the 2Ph-Cu complex could be 6.5 kcal mol−1 more stable than 1Ph-Cu (calculation details are found in the ESI†).

Simultaneously to this Ullmann derivatization study, we studied the acylation of pyrazolo[3,4-b]pyridin-6-ones (13) also with unexpected results. Initially, we treated 2H-13c (obtained upon treatment of pyridone 12c with hydrazine in MeOH under microwave irradiation, Scheme 2) with 1 equivalent of benzoyl chloride and 1.5 equivalents of Et3N at room temperature for 24 h in THF or 1,4-dioxane following the reaction conditions previously described.9 The reaction afforded a mixture of two compounds in a 80 : 20 ratio (1H-NMR integration) that present the same number and type of signals. Both compounds were initially assigned as the N1-benzoyl and N2-benzoyl substituted compounds 1Bz-17c and 2Bz-17c, respectively (Scheme 3).

Interestingly, the ratio of the two compounds changed with the reaction temperature from 80 : 20 at room temperature to 15 : 85 at 200 °C (temperatures higher than 100 °C were achieved by using 1,4-dioxane heated under microwave irradiation and working in a sealed vial) (Fig. 5). For the experiments at 25 °C, 40 °C and 60 °C, the use of THF or 1,4-dioxane showed equivalent results.

Both isomers, 1Bz-17c and 2Bz-17c, were obtained separately by working at different temperatures and purifying the samples by column chromatography.

Surprisingly, isomer 1Bz-17c was transformed to isomer 2Bz-17c when heated at high temperatures (180 °C). Thus, a mixture containing mainly the N1-isomer 1Bz-17c was heated in 1,4-dioxane at 180 °C under microwave irradiation for 30 minutes with no extra reagents. The final crude product contained a mixture composed mainly of isomer 2Bz-17c.

In order to unequivocally establish the structure of isomers 1Bz-17c and 2Bz-17c, we prepared the 13C labelled N2-substituted compound 13C-2Bz-17c using an alternative synthesis. 13C labelled benzhydrazide was reacted with pyridone 12c in CH2Cl2 at 140 °C under microwave irradiation (Scheme 4).

The structure was assigned using the HMBC spectrum of product 13C-2Bz-17c (Fig. 6) where a correlation between the NH2 at C3 and the 13C of the carbonyl group of the benzoyl moiety proved the proximity (4 bond distance) of these two groups.

Finally, the structure of 2Bz-17c could be confirmed by single crystal X-ray diffraction (Fig. 7).

The results above suggest that the behaviour of the reaction may correspond to a kinetic vs. thermodynamic control20 where isomer 1Bz-17c corresponds to the kinetic isomer (the one with the lowest activation energy) and isomer 2Bz-17c to the thermodynamic isomer (the one with the highest

activation energy barrier but the most thermodynamically stable one). A similar situation in aminopyrazoles was described by Fandrick et al.21

With the aim of giving theoretical support to this hypothesis, we calculated22,23 the free-energy path for both possible transformations. The energy values obtained clearly indicate that 2H-13d (R = H) is approximately 2.7 kcal mol−1 more stable than 1H-13d supporting our hypothesis. Moreover, the resulting energy plots as a function of the reaction coordinate have allowed the determination of the energies of the transition states (18d and 19d) and the reaction products (1Bz-17d and 2Bz-17d). The reaction occurs through the practically simultaneous formation of the amide bond and the loss of HCl via a quasi-five membered ring. The results obtained are summarized in Scheme 5.

As it can be seen, the results obtained seemed to validate our hypothesis of a kinetic vs. thermodynamic control where 2H-13d is transformed at low temperature ($\Delta G‡$ = 13.2 kcal mol−1) to the N1-benzoyl isomer 1Bz-17d while at higher temperatures it is transformed (via 1H-13d) through a less stable transition state ($\Delta G‡$ = 14.4 kcal mol−1) to the N2-benzoyl isomer 2Bz-17d, 1.0 kcal mol−1 more stable than 1Bz-17d.

The previous results draw a picture of the reactivity of pyrazolo[3,4-b]pyridin-6-ones 13 (Scheme 6). The most stable tautomer 2H-13 reacts through the NH group (depicted in green) in the Ullmann reaction to afford the N2-phenyl substituted isomer 2Ph-14 while the lone pair of the N1 atom (depicted in blue) reacts in the acylation at room temperature to afford the N1-benzoyl substituted compound 1Bz-17 (kinetic isomer). An increase in the reaction temperature shifts the tautomerization ratio towards the less stable tautomer 1H-13 whose N2 atom (depicted in red) reacts with the benzoyl chloride to afford the N2-benzoyl substituted compound 2Bz-17 (thermodynamic isomer).

The transposition of the 1-benzoyl derivative 1Bz-17 to the more stable 2-benzoyl substituted isomer 2Bz-17 at 180 °C in 1,4-dioxane under microwave irradiation could, probably, follow a mechanism similar to that established for the Fries rearrangement24 or proceed via a N1–N2 triangular transition state in a [1,5]-sigmatropic rearrangement (a calculation suggests a $\Delta G‡$ = 33.5 kcal mol−1 perhaps affordable at 180 °C).

Once established a rationalization to justify the regioselectivity of the Ullmann and acylation reactions of structures 13, we considered if it was possible to extend it to the other structures that contain the pyrazol-3-amino moiety. With this aim, we calculated the energies of the 1H- and 2H-tautomers of the most common pyrazol-3-amines and the ΔG between both tautomers using DFT (Fig. 8).

The values obtained clearly indicate that the degree of unsaturation of the C4–C5 fused ring and the electronic characteristics of such ring determines the ΔG between both tautomers and the most stable tautomer in each case. Thus, while in the not fused pyrazol-3-amine 6 the 1H-tautomer is more stable than the 2H-tautomer by 2.6 kcal mol−1, the situation is totally reversed for our compounds 13 where the 2H-tautomer is 2.1 kcal mol−1 more stable. The introduction of a double bond at the pyridone ring of compounds 13, as it happens in structures 15, balances the relative stability between the two tautomers (0.3 kcal mol−1), hampering a clear identification of the most stable form. The aromatization of the

pyridine ring as it happens in structure 20 will cause the total inversion of the most stable tautomer, now being 1H-20 9.4 kcal mol−1 more stable than 2H-20.

For the rest of C4–C5 fused pyrazol-3-amines considered, 4,5,6,7-tetrahydro-1H-indazol-3-amines (7), 1H-indazol-3-amines (8), and 1H-pyrazolo[3,4-b]pyridin-3-amines (9), the 1Htautomer is always the most stable.

It is interesting to note that presence of a C4–C5 fused aromatic ring as in 20, 8, and 9 largely increases the value of the ΔG in favour of the 1H-tautomer (9.4, 7.9, and 11.1 kcal mol−1, respectively) a fact that correlates with the reactivity of such structures as it will be discussed later.

In order to cast light on the reactivity of such systems and be capable of predicting Ullmann and acylation reactions in the future, we decided to review the information contained in the literature for those structures in Fig. 8 for which such information is available, and to carry out extra experimentation with the other ones.

As described previously in this paper, in the case of the pyrazol-3-amine 6 the references available indicate that the Ullmann reaction takes place mainly at N1 with yields higher than 80%10,11 while the acylation seems to take place at N1 or at N2.12,13 Such result seems to agree with the greater stability of tautomer 1H-6 and the energy difference between both tautomeric forms (1H-6 and 2H-6).

In the case of our compounds 13, the situation is totally reversed and as described above the Ullmann reaction takes place at N2 to afford only compounds 2Ph-14 while the acylation initially produces the N1-acylated compounds 1Bz-17. As discussed previously, such results are caused by the greater stability of the 2H-13.

The introduction of a double bond at the pyridone ring of 2H-13b affords 15b (due to the slight energy difference between both tautomers it is difficult to envisage which one is obtained). The treatment of 15b under Ullmann conditions renders a mixture of isomers 2Ph-16b and 1Ph-16b where the N2-aryl substituted derivative 2Ph-16b is still the major product but allowing the synthesis of the N1-aryl substituted derivative 1Ph-16b in low yield. The benzoylation reaction of 15b has also afforded a mixture of two compounds presenting the same pattern of signals in the 1H-NMR spectrum. The major compound (70% by NMR integration) seems to correspond to the N2-benzoyl substituted isomer 2Bz-21b (Fig. 9) on the basis of the NH2 chemical shift compared with 2Bz-17c. In this case, the very small energy difference between the two possible tautomers 2H-15b and 1H-15b allows an intermediate behaviour between 13 and 6.

To see the effect of the aromatization of the pyridone ring present in our compounds 13, we obtained compound 20 (Fig. 9) upon treatment of the commercially available 2,6-dichloronicotinonitrile with NaOMe/MeOH that yielded a mixture of the 2-methoxy and 6-methoxy substituted chloro nicotinonitriles which were subsequently treated with hydrazine monohydrate to afford 1H-20 (40% yield) as the only bicyclic compound. The Ullmann reaction on 1H-20 only afforded the N1-substituted compound 1Ph-22 (Fig. 9) totally reversing the behaviour observed for the non-aromatic structures 13 and 15. On the other hand, the acylation of 1H-20 afforded a single major compound that corresponds to the

benzamide 23 (Fig. 9) formed by acylation of the NH2 group. Such behaviour must be due to the big difference of stability in favour of the 1H-tautomer of 20.

To the best of our knowledge, no Ullmann reactions have been described for the 4,5,6,7-tetrahydro-1H-indazol-3-amine 7 and, as described in the introduction, there are examples of acylation at both N1 and N2.14

Finally, in the case of compound 8, the aromatic equivalent of compound 7, the Ullmann reaction with iodobenzene leads only to the N1-phenyl substituted compound 1Ph-24 (the substitution point was corroborated by 1D-NOESY spectroscopy). Interestingly, benzoylation of 8 only affords one major product which corresponds to the substitution on the amine group (25, Fig. 9). Once more, the big difference of energy between the two possible tautomers 1H-8 and 2H-8 seems to be the responsible of these results.

Surprisingly, when the pyrazol-3-amine ring is fused to an aromatic ring the acylation reaction only takes place on the NH2 group. Acylation at N1 or N2 of the bicyclic heterocycle would disrupt de 10π aromatic system, whereas acylation of the exocyclic NH2 group does not (Fig. 10).

Thus, the N1 substituted isomers 1R-8 and 1R-9 present aromatic circulation in both rings thanks to the double bond that can be drawn in the fusion of both rings. On the contrary, in the case of the N2 substituted structures 2R-8 and 2R-9 only a peripheric circulation is possible due to the forced positions of the double bonds in the pyrazole ring. Therefore, the aromatic circulation seems to have a remarkable impact on the relative stability of the tautomers and the reactivity of such compounds, being the 1R isomers with a bicyclic aromatic circulation the most stable ones.

CONCLUSIONS

The experimental results obtained in this study combined with the calculations carried out seem to cast light on the uncertainty present in the literature regarding the Ullmann and acylation reactions of C4–C5 fused pyrazol-3-amines. The nitrogen atom of the pyrazole ring in which the Ullmann reaction takes place corresponds to the nitrogen bearing the proton (the NH group) while, preferably, the acylation takes place on the non-protonated nitrogen atom. Such nitrogen atoms (protonated and non-protonated) correspond to the most stable tautomer which can be easily predicted using DFT calculations. In cases in which the energy difference is high (probably above 5 kcal mol−1) the regioselectivity is also high. However, lower energy differences can produce mixtures of regioisomers or even behaviours like the kinetic vs. thermodynamic control found for compounds 13.

When the pyrazol-3-amine ring is fused to an aromatic ring, the difference in favour of the 1H-tautomer is so high (even greater than 10 kcal mol−1) that the Ullmann reaction is regiospecific at N1 and the acylation only takes place in the NH2 group avoiding the alteration of the aromatic conjugation of the bicycle.

In summary, the regioselectivity of the Ullmann and acylation reactions on C4–C5 fused pyrazol-3-amines is controlled by the degree of unsaturation and electronic characteristics of the fused ring. These reactions take place predominantly at the NH group and the non-protonated nitrogen atom, respectively, of the pyrazole ring of the most stable tautomer (1H- or 2H-pyrazol-3-amine) that can be easily predicted using DFT calculations. The complementary derivatization of the less stable tautomer may become practically impossible when the energy difference between both tautomers is high.

In a word, it is worthwhile to determine the energy difference of the two possible tautomeric forms of the pyrazol-3-amine ring before starting an expensive group of experiments that can lead to the undesired final isomer (sometimes difficult to be unequivocally assigned using standard spectroscopic techniques as can be seen above).

EXPERIMENTAL

General information

All solvents and chemicals were reagent grade. Unless otherwise mentioned, all solvents and chemicals were purchased from commercial vendors (Sigma-Aldrich, ABCR, Fluorochem and ACROS Organics) and used without purification. 1H and 13C-NMR spectra were recorded on a Varian 400-MR spectrometer (1H-NMR at 400 MHz and 13C-NMR at 100.6 MHz). Chemical shifts were reported in parts per million (δ) and are referenced to the residual signal of the solvent DMSO-d6 (2.5 ppm in 1H-NMR and 39.5 ppm in 13C-NMR). Coupling constants are reported in Hertz (Hz). Standard and peak multiplicities are designed as follows: s, singlet; d, doublet; dd, doublet of doublets; dt, doublet of triplets t, triplet; q, quadruplet; qn, quintuplet; br, broad signal. IR spectra were recorded in a Thermo Scientific Nicolet iS10 FTIR spectrophotometer with Smart iTr. Wavenumbers (ν) are expressed in cm−1. MS data (m/z (%), EI, 70 eV) were obtained by using an Agilent Technologies 5975. HRMS data were obtained by using a micrOTOF (Bunker) high resolution spectrometer (EI or APCI mode). Elemental microanalyses were obtained on a EuroVector Instruments Euro EA 3000 elemental analyzer. The melting points were determined with a SMP3 melting point apparatus (Stuart Scientific) and are uncorrected. Automatic flash chromatography was performed in an Isco Combiflash medium pressure liquid chromatograph with RediSep® silica gel columns (35–70 μm) using a suitable mixture of solvents as eluent. Microwave irradiation experiments were carried out in an Initiator™ (Biotage) microwave apparatus, operating at a frequency of 2.45 GHz with continuous irradiation power from 0 to 400 W. Reactions were carried out in 2.5, 5, and 20 Ml glass tubes, sealed with aluminium/Teflon crimp tops, which can be exposed up to 250 °C and 20 bar internal pressure. Temperature was measured with an IR sensor on the outer surface of the process vial. After the irradiation period, the reaction vessel was cooled rapidly to 50 °C by air jet cooling. Pyridones 12a (R = Me), 12b (R = Ph), and 12c were synthesized as previously described.8

3-Amino-5-methyl-2,4,5,7-tetrahydro-6H-pyrazolo[3,4-b]pyridin-6-one (2H-13a)

A mixture of 0.60 mmol of pyridone 12a and 1.20 mmol of hydrazine monohydrate in 4 mL of methanol was heated under microwave irradiation at 140 °C for 30 minutes. The solvent was removed under reduced pressure, the residue was dissolved in the minimum amount of methanol and precipitated with ether. The solid was filtered, washed with ether and dried in vacuo over P2O5 to yield 36 mg (36%) of 2H-13a as a white solid. Mp: 246 °C. IR (KBr) νmax (cm−1): 3403 (N–H), 3335 (Csp2–H), 3227, 2930, 1692 (CvO), 1644, 1558, 1540, 1466, 1380, 1286, 798, 712. 1H-NMR (400 MHz, DMSO-d6): δ 10.57 (s, 1H, N–H), 9.83 (s, 1H, N–H), 4.89 (s, 2H, NH2), δ 2.64 (dd, J = 14.8, 6.8 Hz, 1H, C4-H), 2.45–2.34 (m, 1H, C5-H), 2.12 (dd, J = 14.9, 9.6 Hz, 1H, C4-H), 1.09 (d, J = 7.0 Hz, 3H, Me). 13C-NMR (100 MHz, DMSO-d6): δ

173.1 (CvO), 148.4 (C3), 143.4 (C7a), 82.3 (C3a), 35.9 (C5), 23.6 (C4), 16.4 (Me). MS (70 eV, EI): m/z (%): 166.1 (100%), 111.1 (40%), 110.1 (67%), 109.2 (29%), 68.1 (29%), 43.2 (32%). HRMS (EI) m/z calculated for C7H10N4O [M]+: 166.0859; found [M]+: 166.0855.

3-Amino-5-phenyl-2,4,5,7-tetrahydro-6H-pyrazolo[3,4-b]pyridin-6-one (2H-13b)

As above for 2H-13a but using 0.60 mmol of 12b to afford 99 mg (72%) of 2H-13b as a white solid. Mp: >250 °C. IR (KBr), νmax (cm−1): 3348 (N–H), 3230, 1656 (CvO), 1619, 1561, 1381, 701 (Csp2–H). 1H-NMR (400 MHz, DMSO-d6): δ 10.65 (s, 1H, N–H), 10.13 (s, 1H, N–H), 7.31–7.25 (m, 2H, Ph–H), 7.24–7.17(m, 3H, Ph–H, Ph–H), 4.95 (s, 2H, NH2), 3.70 (t, J = 7.2 Hz, 1H, C5-H), 2.83 (dd, J = 15.1, 6.9 Hz, 1H, C4-H), 2.65 (dd, J = 15.1, 7.6 Hz, 1H, C4-H). 13C-RMN (100 MHz, DMSO-d6): δ 171.0 (CvO), 148.3 (C7a), 143.8 (C3), 141.0 (Ph), 128.2 (Ph), 128.1 (Ph), 126.5 (Ph), 81.9 (C3a), 47.6 (C5), 24.1 (C4). MS (70 eV, EI) m/z (%): 228.1 (100%), 137.0 (29%), 110.1 (54%). HRMS (EI) m/z calculated for C12H13N4O+ [M + 1]+: 229.1084; found [M + 1]+: 229.1085.

3-Amino-4-methyl-2,4,5,7-tetrahydro-6H-pyrazolo[3,4-b]pyridin-6-one (2H-13c)

As above for 2H-13a but using 0.60 mmol of 12c to afford 89 mg (89%) of 2H-13c as a white solid. Mp: >250 °C. IR (KBr) νmax (cm−1): 3439 (N–H), 3380 (N–H), 1631, 1680 (CvO). 1H-NMR (400 MHz, DMSO-d6): δ 10.56 (s, 1H, NH), 9.88 (s, 1H, NH), 4.86 (s, 2H, NH2), 2.87 (td, J = 6.8, 4.6 Hz, 1H, C4-H), 2.51 (dd, J = 15.7, 6.8 Hz, 1H, C5-H), 2.10 (dd, J = 15.7, 4.6 Hz, 1H, C5-H), 1.03 (d, J = 6.8 Hz, 3H, Me). 13C-NMR (100 MHz, DMSOd6): δ 170.2 (C1), 147.8, 143.3, 88.1 (C4), 40.4 (C2), 22.5 (C3), 20.9 (C7). MS (70 eV, EI) m/z (%): 166.2 (71%), 152.1 (23%), 151.1 (100%), 148.2 (25%), 136.1 (29%). HRMS (EI) m/z calculated for C7H11N4O+ [M + 1]+: 167.0927; found [M + 1]+: 167.0926.

3-Amino-2,5-diphenyl-2,4,5,7-tetrahydro-6H-pyrazolo[3,4-b] pyridin-6-one (2Ph-14b)

57 mg (0.25 mmol) of 2H-13b, 4.8 mg (0.03 mmol) of CuI, 81.5 mg (0.25 mmol) of Cs2CO3 were placed in a sealable tube reactor equipped with a magnetic stir bar that was sealed in vacuo and flushed with argon. 0.083 mL (0.75 mmol) of iodobenzene in 0.75 mL of N-methyl-2-pyrrolidone (NMP) (previously sealed in vacuo and flushed with argon) were added to the reaction tube using a syringe. The tube was placed in a preheated oil bath and the reaction mixture was stirred at 120 °C for 24 hours and then cooled to room temperature. The mixture was filtered in vacuo through Celite which was washed with DMF. The solvent was removed under reduced pressure and the black residue was suspended in the minimum amount

of water. The resulting precipitate was filtered and washed with water, dried in vacuo over P2O5 to yield 24 mg (31%) of 2Ph-14b. The spectral data were superimposable with those previously reported for 2Ph-14b.8

3-Amino-5-phenyl-2,7-dihydro-6H-pyrazolo[3,4-b]pyridin-6-one (2H-15b or 1H-15b)

50 mg (0.22 mmol) of 2H-13b and 75 mg (0.33 mmol) of 2,3-dichloro-5,6-dicyano-1,4-benzoquinone (DDQ) were dissolved in 4 mL of methanol. The mixture was refluxed for 3 h. Then, the solvent was removed under reduced pressure and the black residue was stirred in ethyl acetate. The solid was filtered and dried in vacuo over P2O5, yielding 41 mg (82%) of 2H-15b (or 1H-15b) as a slightly brown solid. Mp: >250 °C. IR (KBr), νmax (cm−1): 3342 (N–H), 3194 (Csp2–H), 1639 (CvO), 1455, 698 (Csp2–H). 1H-NMR (400 MHz, DMSO-d6): δ 11.26 (s, 1H, N–H), 7.90 (s, 1H, C4-H), 7.57–7.54 (m, 2H, Ph–H), 7.50 (br, 1H, NH), 7.36–7.32 (m, 2H, Ph–H), 7.26–7.20 (m, 1H, Ph–H), 6.06 (s, 2H, NH2). 13C-NMR (100 MHz, DMSO-d6): δ 162.7 (CvO), 147.7 (C7a), 145.3 (C3), 138.4 (Ph), 132.3 (C4), 128.3 (Ph), 127.7 (Ph), 126.1 (Ph), 120.3 (C5), 92.3 (C3a). MS (70 eV, EI) m/z (%): 226.1 (18%), 183.1 (18%), 43.1 (100%). HRMS (ESI): calculated for C12H11N4O+ [M + 1]+: 227.0927; found [M + 1]+: 227.0930.

3-Amino-2,5-diphenyl-2,7-dihydro-6H-pyrazolo[3,4-b]pyridin-6-one (2Ph-16b)

As above for 2Ph-14b but using 40 mg (0.19 mmol) of 2H-15b (or 1H-15b) to yield 13 mg (22%) of 2Ph-16b.

2Ph-16b was also obtained by oxidation of 2Ph-14b: 50 mg (0.16 mmol) of 2Ph-14b and 73 mg (0.32 mmol) of 2,3-dichloro-5,6-dicyano-1,4-benzoquinone (DDQ) were dissolved in 4 mL of methanol. The mixture was stirred at room temperature overnight. The solid was filtered and washed with cold MeOH. The solid obtained was dried in vacuo over phosphorus pentoxide, to yield 34 mg (71%) of 2Ph-16b. IR (KBr): ν (cm−1): 3422 (N–H), 2921 (Ph–H), 1638 (CvO), 1595, 1565 (NH), 702 (Csp2–H). 1H-NMR (400 MHz, DMSO-d6): δ (ppm) 11.40 (s, 1H, NH), 8.02 (s, 1H, C4-H), 7.61–7.57 (m, 3H, N2-Ph), 7.55–7.50 (m, 2H, N2-Ph), 7.39–7.34 (m, 3H, C5-Ph), 7.29–7.22 (m, 2H, C5-Ph), 6.58 (s, 2H, NH2). 13C-NMR (100 MHz, DMSO-d6): δ (ppm) 162.8 (CvO), 148.8 (C7a), 142.9 (C3), 138.6 (N2-Ph), 138.1 (C5), 131.8 (C4), 129.3 (C5-Ph), 128.3 (N2-Ph), 127.7 (C5-Ph), 126.6 (C5-Ph), 126.4 (C5-Ph), 123.2 (N2-Ph), 121.5 (N2-Ph), 93.0 (C3a). MS (70 eV, EI) m/z (%): 303.2 (20%), 302.2 (100%), 301.1 (13%), 237.2 (3%). HRMS (APCI) m/z calculated for C18H15N4O+ [M + 1]+: 303.1240; found [M + 1]+: 303.1239.

3-Amino-1,5-diphenyl-1,7-dihydro-6H-pyrazolo[3,4-b]pyridin-6-one (1Ph-16b)

As above for 2Ph-14b but using 57 mg (0.25 mmol) of 2H-15b (or 1H-15b). After the filtration through Celite, washing with DMF and concentration under reduced pressure, the residue was purified by column chromatography (silica column. Cy : AcOEt gradient 0% to 100% in 5 minutes and then isocratic at 100% AcOEt for 10 minutes). The desired fraction was concentrated in vacuo to afford 16 mg (20%) of 1Ph-16b as a slightly brown solid. Mp: 233–236 °C. IR (KBr), νmax (cm−1): 3426 (N–H), 3304 (Csp2–H), 1632, 1590 (CvO), 1501, 695 (Csp2–H). 1H-NMR (400 MHz, DMSO-d6): δ 11.50 (s, 1H, NH), 8.29–8.21 (m, 2H, N2-Ph), 8.18 (s, 1H, C4-H), 7.61–7.57 (m, 2H, C5-Ph), 7.46–7.41 (m, 4H, C5-Ph, N2-Ph), 7.35–7.31 (m, 1H, C5-Ph), 7.15–7.10 (m, 1H, N2-Ph), 5.99 (s, 2H, NH2). 13C-NMR (100 MHz, DMSO-d6): δ 161.1 (CvO), 149.6 (C7a), 147.9 (C3), 140.0 (N2-Ph), 137.6 (C5-Ph), 132.7 (C4), 129.0 (C5-Ph), 128.8 (C5-Ph), 128.1 (N2-Ph), 126.8 (C5-Ph), 123.2 (N2-Ph), 118.3 (N2-Ph), 116.7 (C5), 104.4 (C3a). MS (70 eV, EI) m/z (%): 303.2 (26%), 302.2 (100%), 301.9 (65%), 77.0 (31%). HRMS (APCI) m/z calculated for C18H15N4O+ [M + 1]+: 303.1240; found [M + 1]+: 303.1238.

3-Amino-1-benzoyl-4-methyl-1,4,5,7-tetrahydro-6H-pyrazolo [3,4-b]pyridin-6-one (1Bz-17c)

37 mg (0.22 mmol) of 2H-13c, 31 mg (0.22 mmol) of benzoyl chloride and 33 mg (0.33 mmol) of Et3N were dissolved in 10 mL of THF. The mixture was stirred at 40 °C overnight. The resulting solid was filtered, and the filtrate was evaporated under reduced pressure. The residue was suspended in MeOH, the solid was removed by filtration and the filtrate was evaporated under reduced pressure. The crude material was purified by column chromatography (silica column. CH2Cl2 : MeOH gradient from 0% to 5% of MeOH for 60 min) to afford 41 mg (69%) of 1Bz-17c as a yellowish solid. Mp: 73–77 °C. IR (KBr), νmax (cm−1): 3342 (N–H), 2923 (Csp2–H), 1667, 1595 (CvO), 1533, 1500, 708 (Csp2–H). 1H-NMR (400 MHz, DMSO-d6): δ 9.60 (s, 1H, NH), 8.01–7.93 (m, 2H, Ph–H), 7.62–7.56 (m, 1H, Ph–H), 7.53–7.45 (m, 2H, Ph–H), 5.73 (s, 2H, NH2), 3.00 (dd, J = 6.9, 2.7 Hz, 1H, C4-H), 2.87 (dd, J = 16.2, 7.4 Hz, 1H, C5-H), 2.33 (dd, J = 16.2, 2.7 Hz, 1H, C5-H), 1.09 (d, J = 6.9 Hz, 3H, Me). 13C-NMR (100 MHz, DMSO-d6): δ 169.0 (CvO), 166.8 (Ph–CvO), 154.8, 140.8, 132.8 (Ph), 132.0 (Ph), 130.3 (Ph), 127.8 (Ph), 97.5 (C3a), 38.7 (C5), 22.4 (C4), 19.8 (Me). MS (70 eV, EI) m/z (%): 270.2 (33%), 105.2 (100%). HRMS (APCI) m/z calculated for C14H15N4O2 + [M + 1]+: 271.1190; found [M + 1]+: 271.1190.

3-Amino-2-benzoyl-4-methyl-2,4,5,7-tetrahydro-6H-pyrazolo [3,4-b]pyridin-6-one (2Bz-17c)

As above for 1Bz-17c but heating 30 minutes under microwave irradiation at 180 °C to afford 23.8 mg (40%) of 2Bz-17c as a white solid.

2Bz-17c was also obtained by cyclization of 12c with benzhydrazide: 0.26 mmol of 12c and 0.51 mmol of benzhydrazide were suspended in 4 mL of CH2Cl2 in a 5 mL microwave vial. The mixture was heated under microwave irradiation for 2 h at 140 °C. The solution was washed with H2O (3 × 5 mL) and the organic layer was dried with MgSO4. The solvent was removed under reduced pressure to afford 30 mg of 2Bz-17c (42%). Mp: 75–80 °C. IR (KBr), νmax (cm−1): 3447 (N–H), 3336 (Csp2–H), 1669, 1595 (CvO), 1546, 1500, 706 (Csp2–H). 1H-NMR (400 MHz, DMSO-d6): δ 10.44 (s, 1H, NH), 7.87–7.80 (m, 2H, Ph–H), 7.60–7.52 (m, 1H, Ph–H), 7.51–7.43 (m, 2H, Ph–H), 6.77 (s, 2H, NH2), 3.05 (pd, J = 6.9, 6.9, 3.1, 1H, C4-H), 2.67 (dd, J = 16.0, 6.9 Hz, 1H, C5-H), 2.21 (dd, J = 16.0, 3.1 Hz, 1H, C5-H), 1.08 (d, J = 6.9, 3H, Me). 13C-NMR (100 MHz, DMSO-d6): δ 170.5 (CvO), 169.4 (Ph–CvO), 152.0, 146.6, 133.9 (Ph), 131.5 (Ph), 139.8 (Ph), 127.7 (Ph), 89.8 (C3a), 39.2 (C5), 21.7 (C4), 20.2 (Me). MS (70 eV, EI) m/z (%): 270.15 (41%), 105.10 (100%), 77.1(31%). HRMS (TOF) m/z (%): calculated for C14H15N4O2 +, [M + 1]+: 270.1190; found [M + 1]+: 271.1190.

13C labelled 3-amino-2-benzoyl-4-methyl-2,4,5,7-tetrahydro-6Hpyrazolo[3,4-b]pyridin-6-one (13C-2Bz-17c)

150 mg (1.2 mmol) of α-13C-benzoic acid and 48 µL (0.66 mmol) of SOCl2 were added into a 5 mL microwave vial with 4 mL of EtOH. The mixture was heated under microwave irradiation for 30 min at 100 °C. The solvent was removed under reduced pressure to eliminate the excess of SOCl2. The crude was dissolved with 4 mL of EtOH and 480 µL (9.9 mmol) of hydrazine monohydrate were added into the solution. The mixture was heated under microwave irradiation for 10 min at 100 °C and the solvent was removed under reduced pressure. The crude was resuspended in diethyl ether to yield 97 mg (57%) of the pure 13C-benzhydrazide as white crystals. 1H-NMR (400 MHz, DMSO-d6): δ 9.75 (s, 1H, NH), 7.84–7.78 (m, 2H, Ph–H), 7.54–7.48 (m, 1H, Ph–H), 7.47–7.41 (m, 2H, Ph–H), 4.45 (s, 2H, NH2).

44 mg (0.26 mmol) of 12c and 70 mg (0.51 mmol) of 13Cbenzhydrazide were suspended in 4 mL of CH2Cl2 in a 5 mL microwave vial. The mixture was heated under microwave irradiation for 2 h at 140 °C. The crude was purified by column chromatography (silica column, cyclohexane : AcOEt gradient 0–50% in 10 minutes and then isocratic 50 : 50 for 30 minutes) to afford 14 mg (19%) of 13C-2Bz-17c as a yellowish solid. 1H-NMR (400 MHz, DMSO-d6): δ 10.44 (s, 1H, NH), 7.92–7.77 (m, 2H, Ph–H), 7.63–7.52 (m, 1H, Ph–H), 7.52–7.40 (m, 2H, Ph–H), 6.77 (s, 2H, NH2), 3.06 (td, J = 6.9, 6.9, 3.1, 1H, C4-H), 2.67 (dd, J = 16.0, 6.9 Hz, 1H, C5-H), 2.21 (dd, J = 16.0, 3.1 Hz, 1H, C5-H), 1.08 (d, J = 6.9 Hz, 3H, Me). 13C-NMR (100 MHz, DMSO-d6): δ 170.5 (CvO), 169.4 (13CvO), 152.0 (d, J = 6.1 Hz, C3), 146.6 (d, J = 1.9 Hz, C7a), 133.9 (d, J = 68.6 Hz, Ph), 131.5 (Ph), 129.8 (d, J = 2.3 Hz, Ph), 127.7 (d, J = 4.5 Hz, Ph), 89.8 (C3a), 39.2 (C5), 21.7 (C4), 20.2 (Me).

6-Methoxy-1H-pyrazolo[3,4-b]pyridin-3-amine (1H-20)

400 mg (2.3 mmol) of 2,6-dichloronicotinonitrile were suspended in 20 mL of anhydrous MeOH. 150 mg (2.8 mg) of NaOMe were added and the mixture was refluxed for 24 h. The solvent was removed under reduced pressure and the crude was suspended in water. The solid was filtered and dried in vacuo over P2O5 to yield a mixture of two isomers that was used without further purification.

250 mg of the mixture and 150 mg of hydrazine monohydrate (3 mmol) were dissolved in 20 mL of MeOH and heated under microwave irradiation at 140 °C for 1 h. The solvent was removed under reduced pressure, the residue was dissolved in the minimum amount of methanol and precipitated with ether. The solid was filtered and dried in vacuo over P2O5 to yield 100 mg (40%) of 1H-20 as a yellowish solid. Mp: 196–198 °C. IR (KBr), νmax (cm−1): 3386 (N–H), 3306 (N–H), 3214, 1625 (Csp2–Csp2), 1602, 1519, 1446, 1412, 1334 (C–O), 1256, 1030, 802 (Csp2–H). 1H-NMR (400 MHz, DMSO-d6): δ 11.70 (s, 1H, NH), 7.94 (d, J = 8.5 Hz, 1H, C4-H), 6.38 (d, J = 8.5 Hz, 1H, C5-H), 5.36 (s, 2H, NH2), 3.85 (s, 3H, Me). 13C-NMR (100 MHz, DMSO-d6): δ 163.5 (C6), 150.8, 148.3, 132.2 (C4), 102.6 (C5), 100.8 (C3a), 53.1 (Me). MS (70 eV, EI) m/z (%): 165.1 (10%), 164.1 (100%), 163.1 (26%), 135.1 (13%), 64.1 (3%). HRMS (APCI): calculated for C7H9N4O+ [M + 1]+: 165.0771; found [M + 1]+: 165.0769.

3-Amino-2-benzoyl-5-phenyl-2,7-dihydro-6H-pyrazolo[3,4-b] pyridin-6-one (2Bz-21b)

As above for 1Bz-17c but using 80 mg (0.35 mmol) of 15b. The crude material was purified by column chromatography (silica column. Cy : AcOEt gradient from 0% to 50% of AcOEt for 30 min) to afford 10 mg (9%) of 2Bz-21b as a yellowish solid. Mp: 215–218 °C. IR (KBr), νmax (cm−1): 3431 (N–H), 3391 (N–H), 1687 (CvO), 1660, 1608 (Csp2–Csp2), 1376 (C–O), 1295 1H-NMR (400 MHz, DMSO-d6): δ 11.42 (s, 1H, NH), 8.04 (s, 1H, C4-H), 8.00 (s, 2H, NH2), 7.97–7.93 (m, 2H, PhCO), 7.64–7.60 (m, 1H, PhCO), 7.57–7.50 (m, 4H, PhCO, Ph), 7.40–7.34 (m, 2H, Ph), 7.31–7.25 (m, 1H, Ph). 13C-NMR (100 MHz, DMSO-d6): δ 170.0 (CvO–Ph), 163.3 (CvO), 150.9 (C3), 148.1 (C3b), 137.4 (Ph), 133.4 (Ph–CO), 132.0 (Ph–CO), 131.1 (C4), 130.2 (Ph–CO), 128.4, 127.8, 127.8, 126.8 (Ph), 123.0 (C5), 91.3 (C3a). MS (70 eV, EI) m/z (%): 331.2 (27%), 330.2 (100%), 226.2 (10%), 105.1 (68%), 51.1 (9%). HRMS (APCI): calculated for C19H15N4O2 + [M + 1]+: 331.1190; found [M + 1]+: 331.1187.

6-Methoxy-1-phenyl-1H-pyrazolo[3,4-b]pyridin-3-amine (1Ph-22)

As above for 2Ph-14b but using 50 mg (0.30 mmol) of 1H-20 and increasing reaction time to 96 h. 30 mg of 1Ph-22 (42%) are obtained as a brown solid. Mp: 160–162 °C. IR (KBr), νmax (cm−1): 3401 (N–H), 2942, 1606 (Csp2–Csp2), 1595, 1495, 1446, 1408, 1335 (C–O), 1290, 1215, 1020, 755, 691. 1H-NMR

(400 MHz, DMSO-d6): δ 8.27–8.18 (m, 2H, Ph), 8.12 (d, J = 8.6 Hz, 1H, C4-H), 7.49–7.40 (m, 2H, Ph), 7.17–7.08 (m, 1H, Ph), 6.60 (d, J = 8.6 Hz, 1H, C5-H), 6.00 (s, 2H, NH2), 3.98 (s, 3H, Me). 13C-NMR (100 MHz, DMSO-d6): δ 163.9 (C6), 149.2, 148.5, 139.9 (Ph), 133.0 (C4), 128.9 (Ph), 123.2 (Ph), 118.0 (Ph), 110.3 (C3a), 104.1 (C5), 53.5 (Me). MS (70 eV, EI) m/z (%): 241.2 (16%), 240.2 (100%), 239.2 (18%), 194.2 (5%). HRMS (APCI): calculated for C13H13N4O+ [M + 1]+: 241.1084; found [M + 1]+: 241.1081.

N-(6-Methoxy-1H-pyrazolo[3,4-b]pyridin-3-yl)benzamide (23)

As above for 1Bz-17c but using 100 mg (0.61 mmol) of 1H-20. The crude material was purified by column chromatography (silica column. Cy : AcOEt gradient from 0% to 100% of AcOEt for 32 min) to afford 43 mg (26%) of 23 as a white solid. Mp: 244–246 °C. IR (KBr), νmax (cm−1): 3276 (N–H), 3183, 1646 (CvO), 1615, 1593 (N–H), 1541 (Csp2–Csp2), 1439, 1405, 1329 (C–O), 1246, 1027, 688 (Csp2–H). 1H-NMR (400 MHz, DMSOd6): δ 13.07 (s, 1H, N1-H), 10.94 (s, 1H, NH), 8.19 (d, J = 8.8 Hz, 1H, C4-H), 8.08–8.04 (m, 2H, Ph), 7.64–7.58 (m, 1H, Ph), 7.57–7.50 (m, 2H, Ph), 6.61 (d, J = 8.8 Hz, 1H, C5-H), 3.93 (s, 3H, Me). 13C-NMR (100 MHz, DMSO-d6): δ 165.2 (CvO), 163.6 (C6), 150.4, 139.8, 135.0 (C4), 133.6 (Ph), 131.9 (Ph), 128.4 (Ph), 127.9 (Ph), 105.6 (C5), 103.5 (C3a), 103.5 (Me). MS (70 eV, EI) m/z (%): 269.1 (19%), 268.2 (100%), 267.2 (9%), 240.2 (35%), 105.2 (38%). HRMS (APCI): calculated for C14H13N4O2 + [M + 1]+: 269.1033; found [M + 1]+: 269.1030.

1-Phenyl-1H-indazol-3-amine (1Ph-24)

As above for 2Ph-14b but using 67 mg (0.5 mmol) of 1Hindazol-3-amine to afford 67 mg (64%) of 1Ph-24. Mp: 84–86 °C. IR (KBr), νmax (cm−1): 3319 (N–H), 3203, 3058 (Csp2–H), 1614 (Csp2–Csp2), 1594, 1540, 1500, 1443, 1422, 1379, 1225, 743 (Csp2–H), 695. 1H-NMR (400 MHz, DMSO-d6): δ 7.84 (ddd, J = 8.0, 0.8 Hz, 1H, C4-H), 7.74 (dt, J = 8.5, 0.8 Hz, 1H, C7-H), 7.70–7.65 (m, 2H, Ph), 7.51–7.45 (m, 2H, Ph), 7.40 (ddd, J = 8.5, 6.9, 1.2 Hz, 1H), 7.22–7.16 (m, 1H, Ph), 7.10 (ddd, J = 7.9, 6.9, 0.8 Hz, 1H), 5.90 (s, 2H, NH2). 13C-NMR (100 MHz, DMSO-d6): δ 151.3 (C3), 140.9 (Ph), 139.7 (C3b), 130.3 (Ph), 129.1 (C6), 125.2 (Ph), 121.6 (C4), 121.0 (Ph), 120.6 (C5), 117.5 (C3a), 110.6 (C7). MS (70 eV, EI) m/z (%): 210.2 (16%), 209.2 (100%), 208.2 (23%), 192.1 (6%), 51.1 (10%). HRMS (EI): calculated for C13H12N3 + [M + 1]+: 210.1026; found [M + 1]+: 210.1023.

N-(1H-Indazol-3-yl)benzamide (25)

As above for 1Bz-17c but using 100 mg (0.75 mmol) of 1Hindazol-3-amine. The crude material was purified by column chromatography (silica column. Cy : AcOEt gradient from 0% to 100% of AcOEt for 30 min) to afford 68 mg (43%) of 25 as a white solid. Mp: 152–153 °C. IR (KBr), νmax (cm−1): 3245 (O–H), 3060 (Csp2–H), 1656 (CvO), 1538, 1349 (C–O), 1281, 746 (Csp2–H), 708. 1H-NMR (400 MHz, DMSO-d6): δ 12.80 (s, 1H, NH), 10.77 (s, 1H, NH), 8.11–8.06 (m, 2H, Ph), 7.72 (dd, J = 8.2, 0.9 Hz, 1H, C4-H), 7.64–7.59 (m, 1H, Ph), 7.58–7.51 (m, 2H, Ph), 7.49 (dt, J = 8.4, 0.9 Hz, 1H, C7-H), 7.36 (ddd, J = 8.4, 6.8, 1.1 Hz, 1H, C6-H), 7.08 (ddd, J = 8.2, 6.8, 0.9 Hz, 1H, C5-H). 13C-NMR (100 MHz, DMSO-d6): δ 165.6 (CvO), 141.1 (C3), 140.1(C3b), 133.8 (Ph), 131.8 (Ph), 128.4 (Ph), 127.9 (Ph), 126.3 (C6), 121.8 (C4), 119.6 (C5), 117.1 (C3a), 110.2 (C7). Elemental analysis: calculated for C14H11N3O: C: 70.87%, H:4.67%, N: 17.71%, found C:70.91%, H: 4.99%, N:17.68%. MS (70 eV, EI) m/z (%): 238.2 (19%), 237.2 (100%), 236.1 (8%), 209.2 (19%), 105.1 (15%), 51.1 (25%). HRMS (APCI): calculated for C14H12N3O+ [M + 1]+: 238.0975; found [M + 1]+: 238.0974.

Quantum mechanics calculations

Energy calculations were carried out using the Gaussian 09 Rev. E.0139. An hybrid non-local density functional theory (DFT), particularly Becke's gradient-corrected exchange–correlation density functional B3LYP with the 6-31 + G(d,p)//6-311++G(d,p) basis set was used for the geometry optimization and the calculation of frequencies.

Mechanistic studies were performed using ORCA v.4.2.1 software: the structures of the molecules under study were constructed using Avogadro molecular editor25 (the two tautomeric pyrazolo[3,4-b]pyridin-6-ones 1H-13d and 2H-13d not bearing any extra substituent at the pyrazole ring, the structures of benzoyl chloride and HCl and the structures of the two benzoyl substituted compounds: N1-benzoyl substituted 1Bz-17d and N2-benzoyl substituted 2Bz-17d). The structures of 1H-13d and 2H-13d were optimized using B3LYP/def2-SVP.

A saddle point (TS) optimization via relaxed scan was carried out starting from both tautomers (1H-13d and 2H-13d) together with the benzoyl chloride initially situated at 3 Å and scanning the distance between the non-protonated pyrazole nitrogen atom (N2 for 1H-13d and N1 for 2H-13d) and the carbon atom of the acid chloride function of the benzoyl chloride from 3.0 to 1.2 Å in 15 points. The resulting energy plots as a function of the reaction coordinate allowed the determination of the energies of the reactants, the transition states (18d and 19d) and the reaction products. The video files of the trajectories are found in the ESI.†

ACKNOWLEDGEMENTS

E. Bou-petit thanks the secretaria d'universitats i recerca del Departament d'economia i coneixement de la generalitat de Catalunya (2017 fi_b2 00139) and the european social funds For her predoctoral fellowship.

NOTES AND REFERENCES

1 J. L. Raoul, M. Gilabert, X. Adhoute and J. Edeline, Expert Opin. Pharmacother., 2017, 18, 1467–1476.

2 L. W. Mohamed, M. A. Shaaban, A. F. Zaher, S. M. Alhamaky and A. M. Elsahar, Bioorg. Chem., 2019, 83, 47–54.

3 I. L. Lu, C. F. Huang, Y. H. Peng, Y. T. Lin, H. P. Hsieh, C. T. Chen, T. W. Lien, H. J. Lee, N. Mahindroo, E. Prakash, A. Yueh, H. Y. Chen, C. M. V. Goparaju, X. Chen, C. C. Liao, Y. S. Chao, J. T.-A. Hsu and S. Y. Wu, J. Med. Chem., 2006, 49, 2703–2712.

4 J. Ducrey and P. Schmidt, Aminobenzenesulfonamide, US2858309, 1958.

5 N. Bodor, M. J. S. Dewar and A. J. Harget, J. Am. Chem. Soc., 1970, 92, 2929–2936.

6 M. Jarończyk, J. C. Dobrowolski and A. P. Mazurek, J. Mol. Struct.: THEOCHEM, 2004, 673, 17–28.

7 A. N. Chermahini and A. Teimouri, J. Chem. Sci., 2014, 126, 273–281.

8 E. Bou-Petit, E. Picas, C. Puigjaner, M. Font-Bardia, N. Ferrer, J. Sempere, R. Puig de la Bellacasa, X. Batllori, J. Teixido, R. Estrada-Tejedor, S. Ramon y. Cajal and J. I. Borrell, ChemistrySelect, 2017, 2, 3668–3672.

9 J. L. Falco, M. Lloveras, I. Buira, J. Teixido, J. I. Borrell, E. Mendez, J. Terencio, A. Palomer and A. Guglietta, Eur. J. Med. Chem., 2005, 40, 1179–1187.

10 A. Beyer, T. Castanheiro, P. Busca and G. Prestat, ChemCatChem, 2015, 7, 2433–2436.

11 K. A. Kumar, P. Kannaboina, D. N. Rao and P. Das, Org. Biomol. Chem., 2016, 14, 8989–8997.

12 S. Tsai and P. Wang, Lipase catalyzed kinetic resolution of azolides, US20110045551, 2011.

13 G. Saxty, V. Berdini, C. W. Murray, C. M. Griffiths-Jones, E. Vickerstaffe, G. E. Besong and M. G. Carr, Bicyclic heterocyclic compounds as selective protein tyrosine kinase inhibitors, their preparation and use in treating cancer and other diseases mediated by FGFR kinase, WO2009047506, 2009.

14 M. P. Ponda, J. L. Breslow, H. Selnick and M. Egbertson, Aminoacylindazoles as immunomodulators for treatment of autoimmune diseases and their preparation, WO2017205296, 2017.

15 J. fu Lu, L. xia Jin, H. guang Ge, J. Song, C. bin Zhao, X. hua Guo, S. yu Yue and L. Li, J. Chem. Res., 2018, 42, 309–312.

16 G. B. Lapa, O. B. Bekker, E. P. Mirchink, V. N. Danilenko and M. N. Preobrazhenskaya, J. Enzyme Inhib. Med. Chem., 2013, 28, 1088–1093.

17 M. Chioua, E. Soriano, A. Samadi and J. Marco-Contelles, J. Heterocycl. Chem., 2010, 47, 861–872.

18 S. Ueda and S. L. Buchwald, Angew. Chem., Int. Ed., 2012, 51, 10364–10367.

19 M. J. Frisch, G. W. Trucks, H. B. Schlegel, G. E. Scuseria, M. A. Robb, J. R. Cheeseman, G. Scalmani, V. Barone, G. A. Petersson, H. Nakatsuji, X. Li, M. Caricato, A. V. Marenich, J. Bloino, B. G. Janesko, R. Gomperts, B. Mennucci, H. P. Hratchian, J. V. Ortiz, A. F. Izmaylov, J. L. Sonnenberg, D. Williams-Young, F. Ding, F. Lipparini, F. Egidi, J. Goings, B. Peng, A. Petrone, T. Henderson, D. Ranasinghe, V. G. Zakrzewski, J. Gao, N. Rega, G. Zheng, W. Liang, M. Hada, M. Ehara, K. Toyota, R. Fukuda, J. Hasegawa, M. Ishida, T. Nakajima, Y. Honda, O. Kitao, H. Nakai, T. Vreven, K. Throssell, J. A. Montgomery Jr., J. E. Peralta, F. Ogliaro, M. J. Bearpark, J. J. Heyd, E. N. Brothers, K. N. Kudin, V. N. Staroverov, T. A. Keith, R. Kobayashi, J. Normand, K. Raghavachari, A. P. Rendell, J. C. Burant, S. S. Iyengar, J. Tomasi, M. Cossi, J. M. Millam, M. Klene, C. Adamo, R. Cammi, J. W. Ochterski, R. L. Martin, K. Morokuma, O. Farkas, J. B. Foresman and D. J. Fox, Gaussian 09, Revision A.02, Gaussian, Inc., Wallingford CT, 2016.

20 K. C. Lin, J. Chem. Educ., 1988, 65, 857–860.

21 D. R. Fandrick, S. Sanyal, J. Kaloko, J. A. Mulder, Y. Wang, L. Wu, H. Lee, F. Roschangar, M. Hoffmann and C. H. Senanayake, Org. Lett., 2015, 17, 2964–2967.

22 F. Neese, Wiley Interdiscip. Rev.: Comput. Mol. Sci., 2012, 2, 73–78.

23 F. Neese, Wiley Interdiscip. Rev.: Comput. Mol. Sci., 2018, 8, e1327.

24 F. Effenberger and R. Gutmann, Chem. Ber., 1982, 115, 1089–1102.

25 M. D. Hanwell, D. E. Curtis, D. C. Lonie, T. Vandermeerschd, E. Zurek and G. R. Hutchison, J. Cheminf., 2012, 4, 17.

Legends to figures

Figure. 1 Structure of pyrazol-3-amines and compounds biologically active bearing such substructure.

Figure 2. Possible tautomeric forms of 1H-pyrazol-3-amine.

Scheme 1. Structures of fused pyrazol-3-amines and synthesis of 3-amino-2,4,5,7-tetrahydro-6H-pyrazolo[3,4-b]pyridin-6-ones (2H-13).

Scheme 2. Reaction conditions used for the Ullmann and acylation reactions on tautomeric C4–C5 fused pyrazol-3-amines.

Figure 3. Structures involved in the derivatization of 3-amino-2,4,5,7-tetrahydro-6H-pyrazolo[3,4-b]pyridin-6-ones by Ullmann reaction.

Figure 4. ORTEP diagram and atomic numbering of 1Ph-16b.

Scheme 3. Synthesis of 3-amino-4-methyl-2,4,5,7-tetrahydro-6H-pyrazolo[3,4-b]pyridin-6-one (2H-13c) and benzoylated derivatives.

Figure. 5. Correlation between isomers 1Bz-17c and 2Bz-17c and the reaction temperature.

Scheme 4. Synthesis of the 13C labelled N2-benzoyl substituted isomer 13C-2Bz-17c.

Figure. 6. HMBC spectrum of 13C-2Bz-17c demonstrating the N2 substitution.

Figure. 7. ORTEP diagram and atomic numbering of 2Bz-17c.

Scheme 5. Kinetic vs. thermodynamic control in acylation of 2H-13d. Energy differences in kcal mol−1. ΔG between tautomers obtained by difference of ΔG‡.

Scheme 6. Reactivity of pyrazolo[3,4-b]pyridin-6-ones 13: Ullmann reaction and acylation (kinetic vs. thermodynamic control).

Figure. 8. Relative stability of the pyrazol-3-amine tautomers.

Figure. 9. Ullmann and acylation products of C4–C5 fused pyrazol-3-amines.

678 **Figure.10.** Aromatic circulation for the N1- and N2-substituted pyrazol-3-amines fused to an aromatic
679 ring.
680
681

FIGURE 1

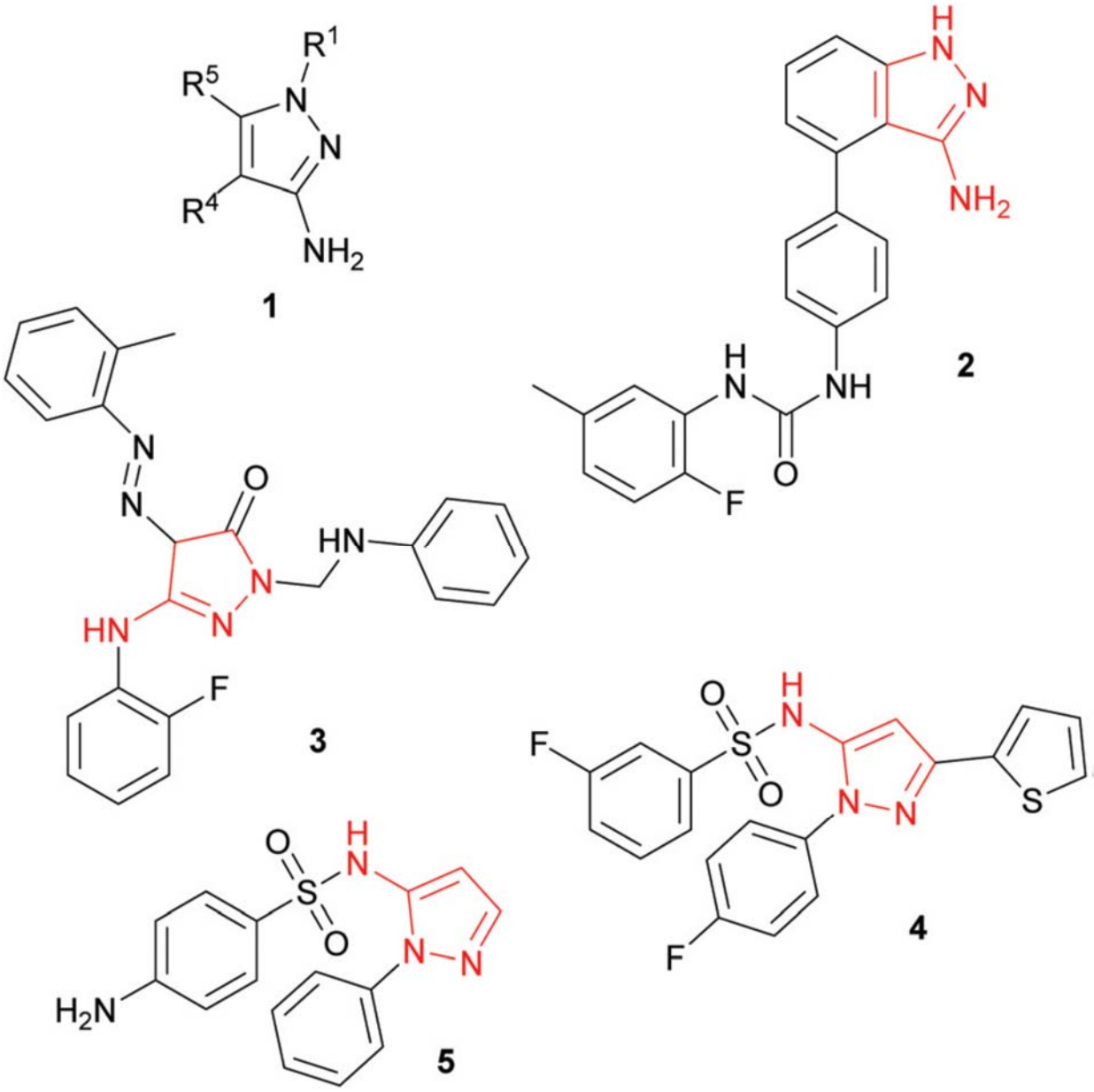
R1
R5
N
N
R4
NH2
1
H
N
N
NH2
2
H
N
NH
O
F
N
N
O
HN
N
HN
N
F
3
O
S
O
H
N
N
N
H2N
5
O
S
O
H
N
F
N
N
S
F
4

FIGURE 2

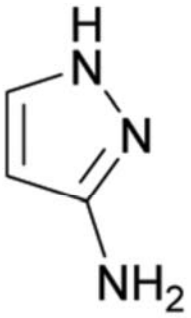

1*H*-**6**

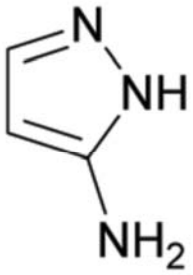

2*H*-**6**

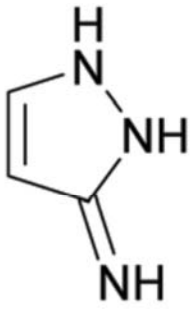

imino-**6**

SCHEME 1

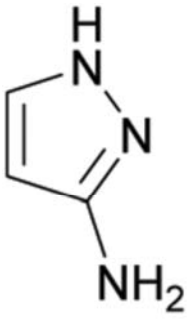

1*H*-**6**

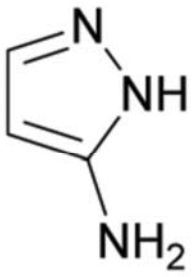

2*H*-**6**

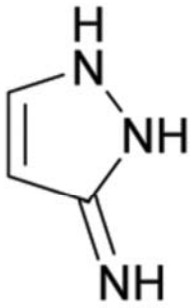

imino-**6**

SCHEME 2

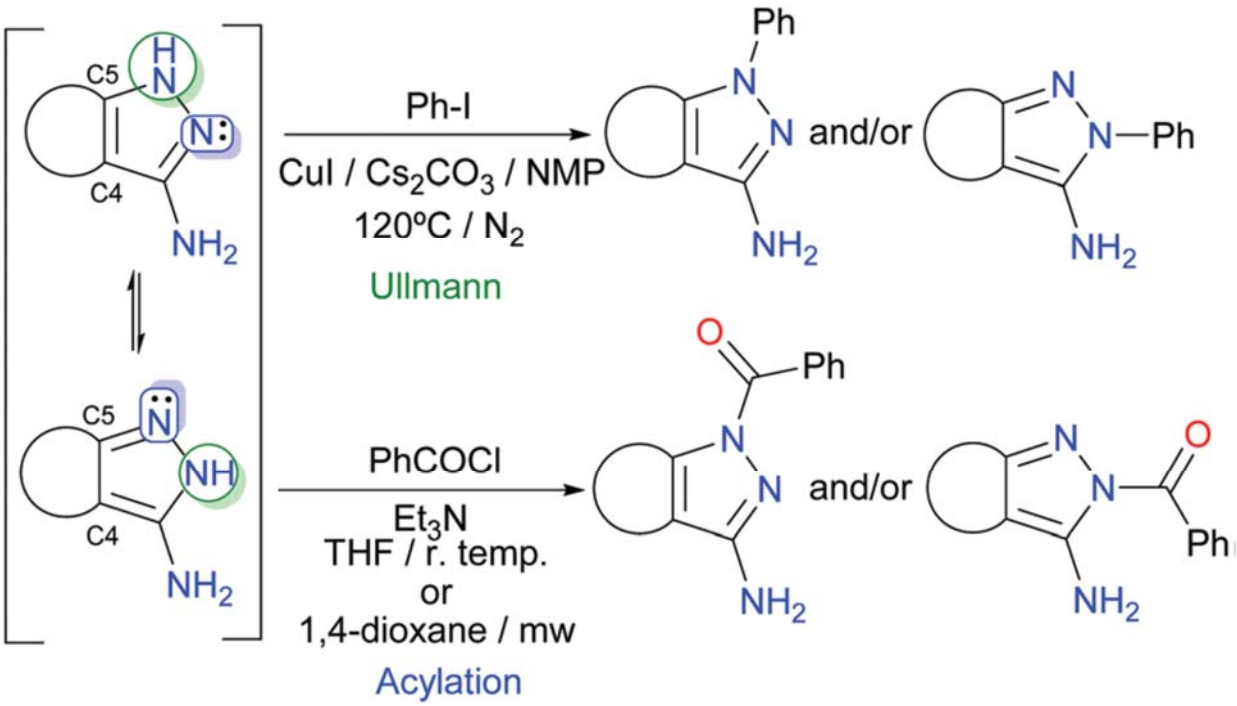
C5
H
N
N:
C4
NH2
Ph-I
CuI / Cs2CO3 / NMP
120ºC / N2
Ullmann
Ph
N
N
NH2
and/or
N
N—Ph
NH2
C5
N
NH
C4
NH2
PhCOCl
Et3N
THF / r. temp.
or
1,4-dioxane / mw
Acylation
O
Ph
N
N
NH2
and/or
N
N
O
Ph
NH2

FIGURE 3

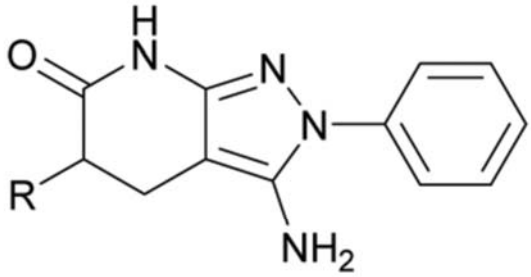

2Ph-**14a**: R = Me

2Ph-**14b**: R = Ph

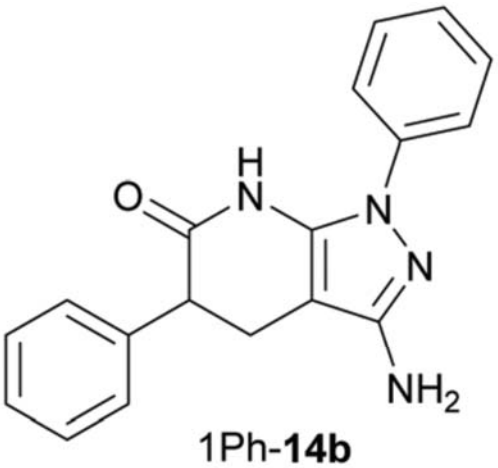

1Ph-**14b**

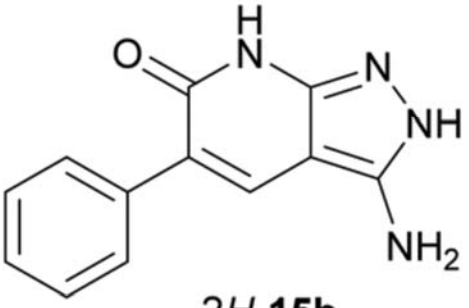

2*H*-**15b**

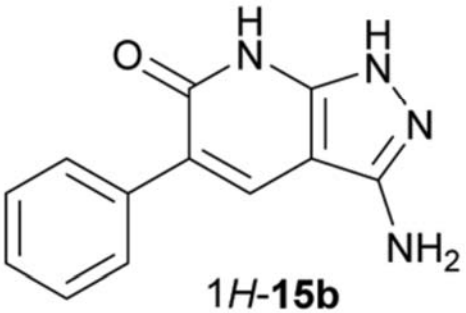

1*H*-**15b**

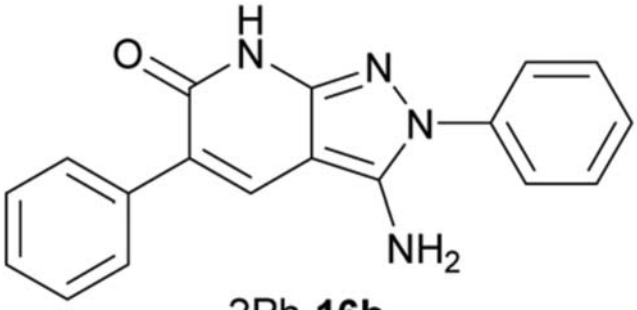

2Ph-**16b**

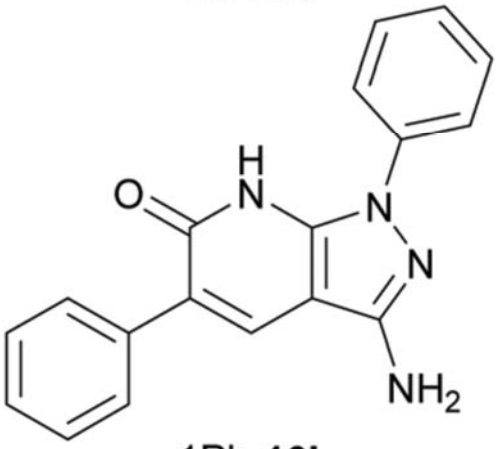

1Ph-**16b**

FIGURE 4

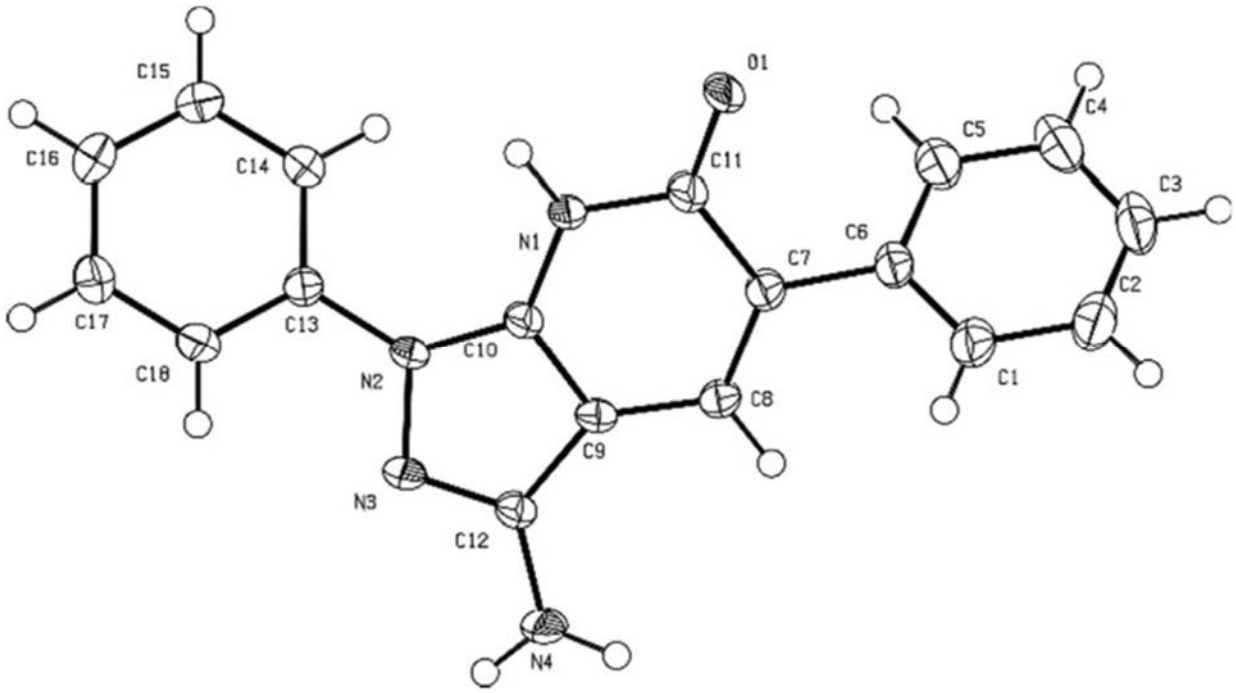
C15
O1
C4
C5
C16
C14
C11
C3
N1
C6
C7
C2
C17
C13
C10
C1
C18
N2
C8
C9
N3
C12
N4

SCHEME 3

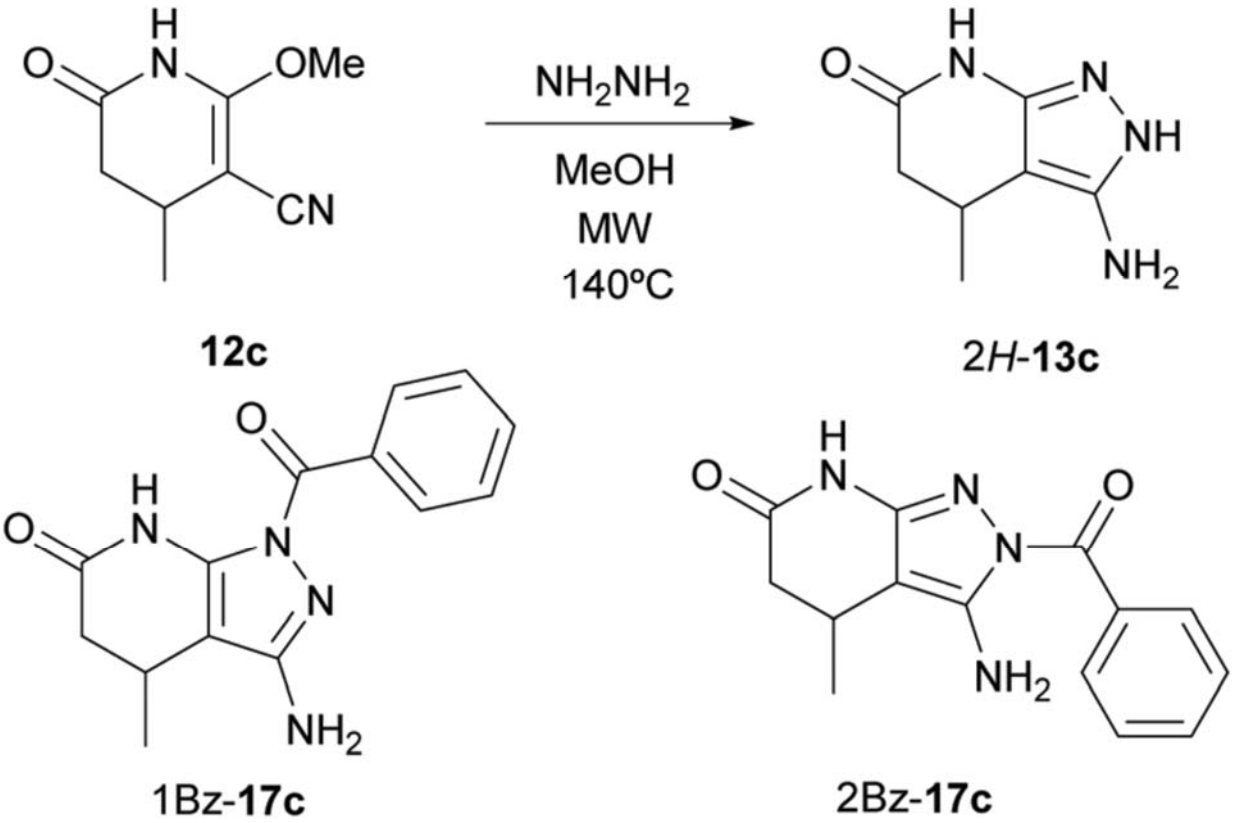
H
N
O
OMe
CN
NH2NH2
MeOH
MW
140°C
N
NH
NH2
12c
2H-13c
1Bz-17c
2Bz-17c

FIGURE 5

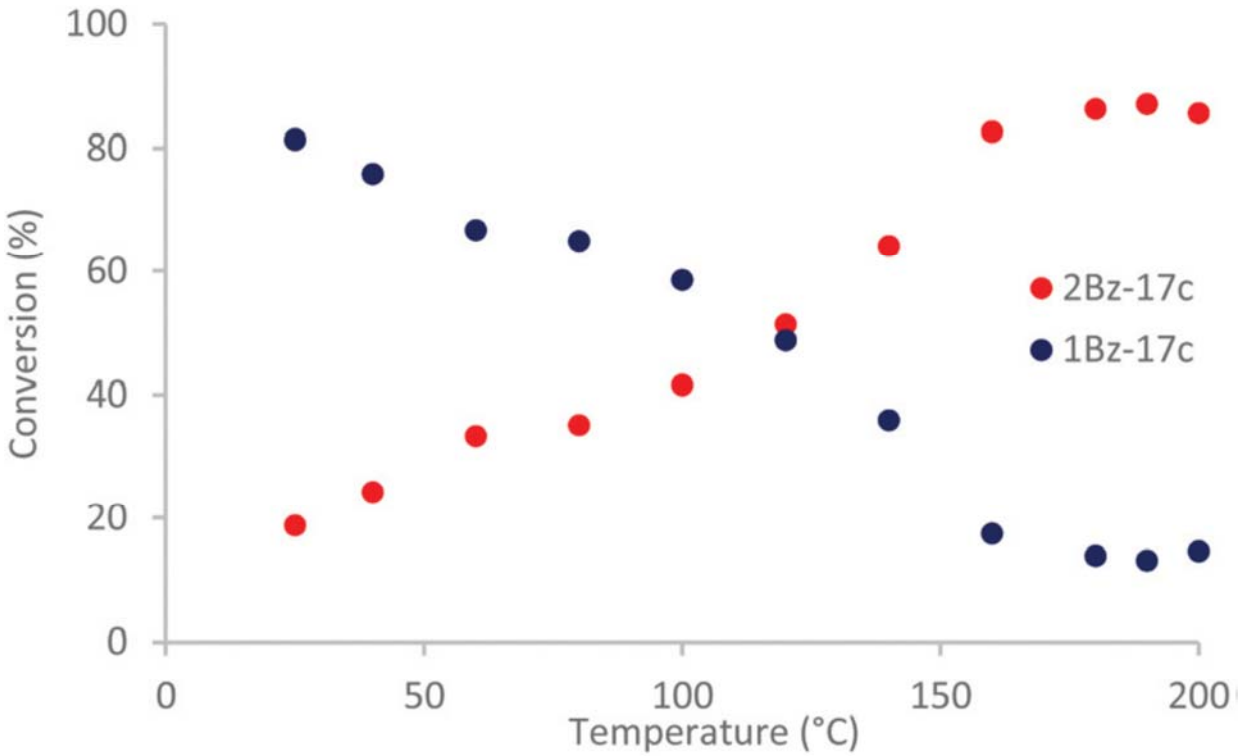
100
80
60
40
20
0
Conversion (%)
0
50
100
150
200
Temperature (°C)
2Bz-17c
1Bz-17c

SCHEME 4

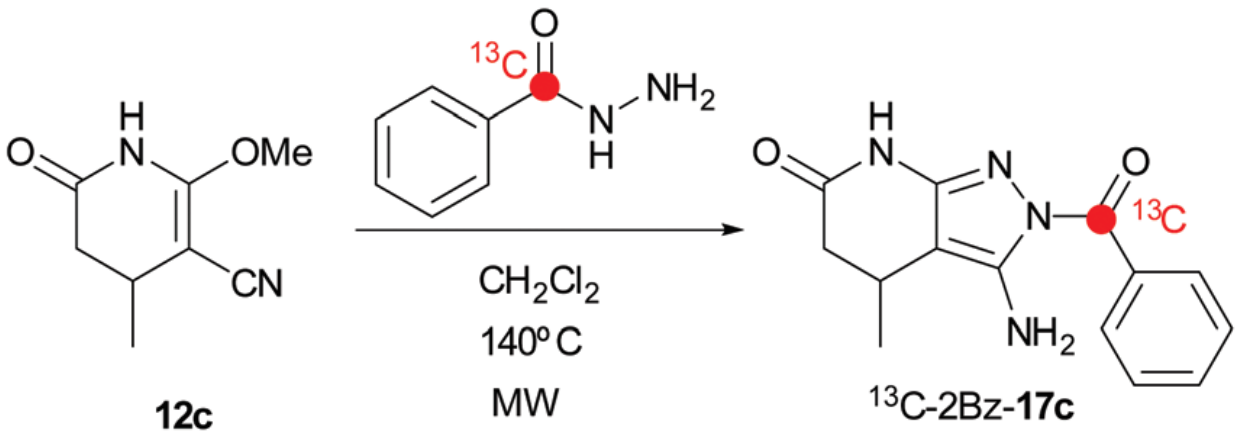
O
H
N
OMe
CN
12c
^{13}C
O
NH$_2$
N
H
CH$_2$Cl$_2$
140° C
MW
H
N
O
N
N
O
^{13}C
NH$_2$
^{13}C-2Bz-17c

FIGURE 6

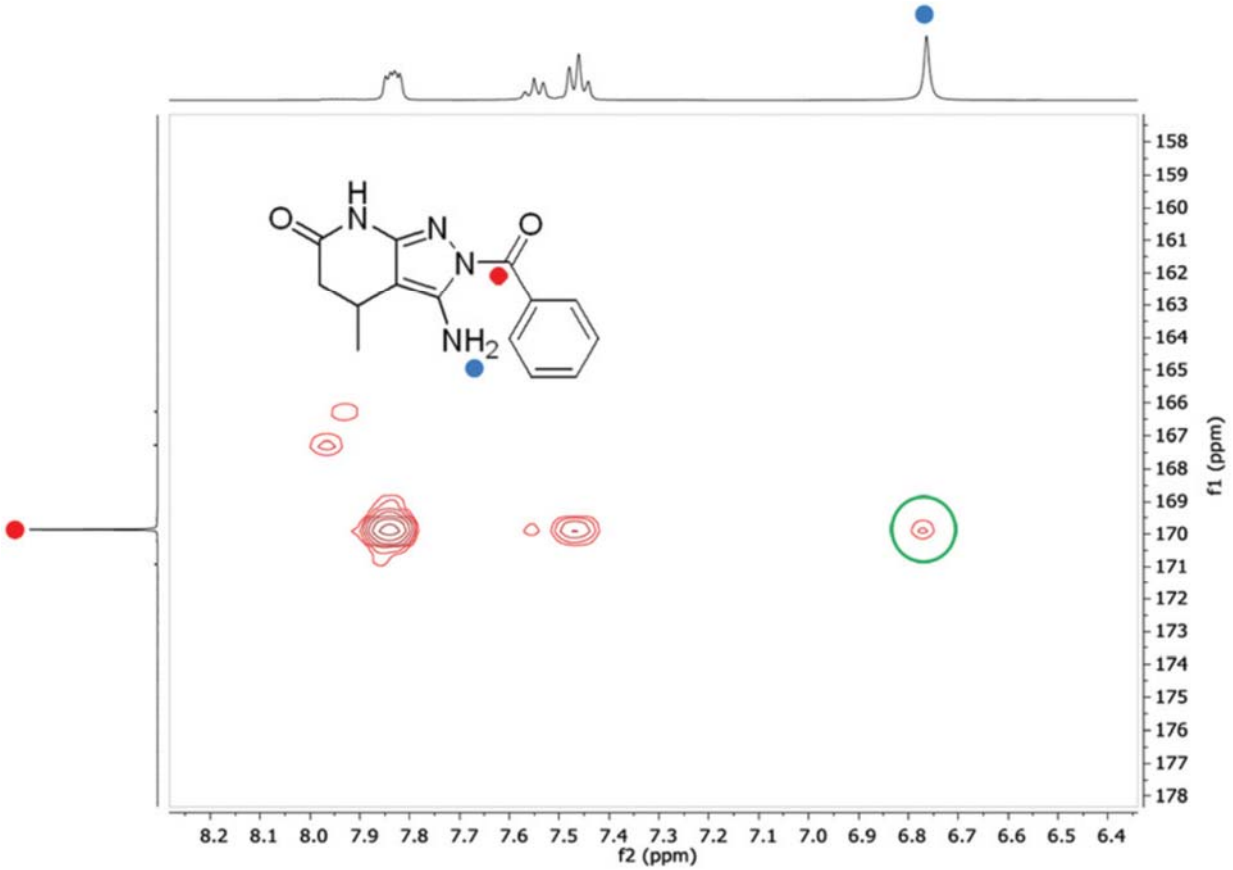
H
N
O
N
N
O
NH2
158
159
160
161
162
163
164
165
166
167
168
169
170
171
172
173
174
175
176
177
178
f1 (ppm)
8.2
8.1
8.0
7.9
7.8
7.7
7.6
7.5
7.4
7.3
7.2
7.1
7.0
6.9
6.8
6.7
6.6
6.5
6.4
f2 (ppm)

FIGURE 7

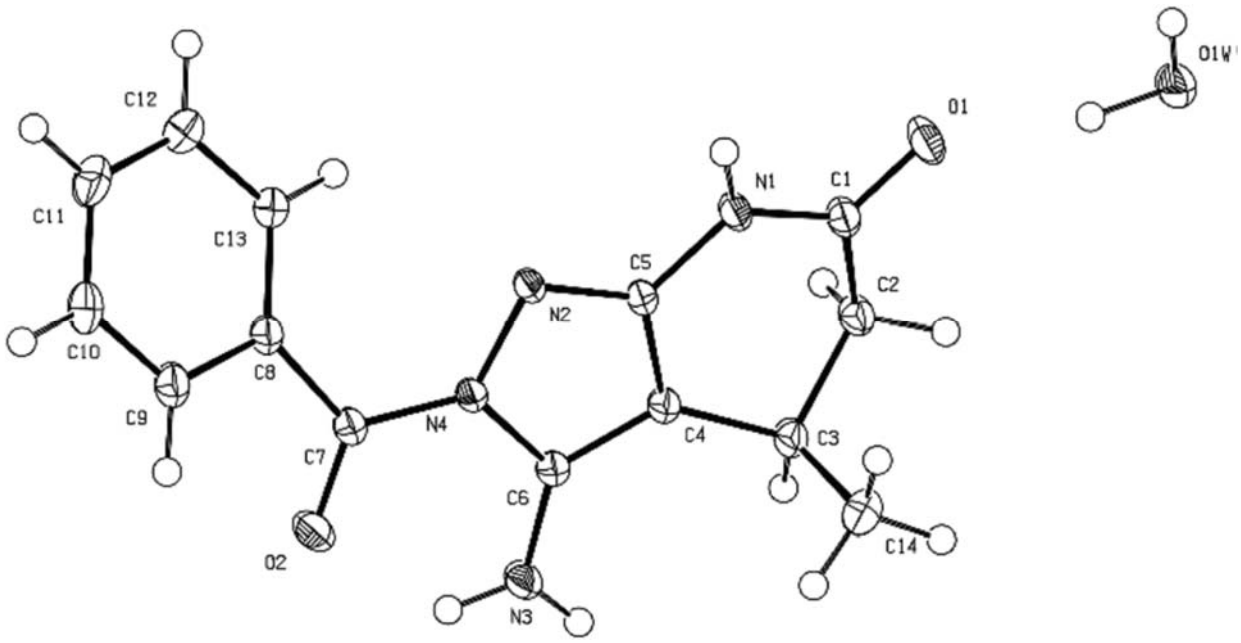

SCHEME 5

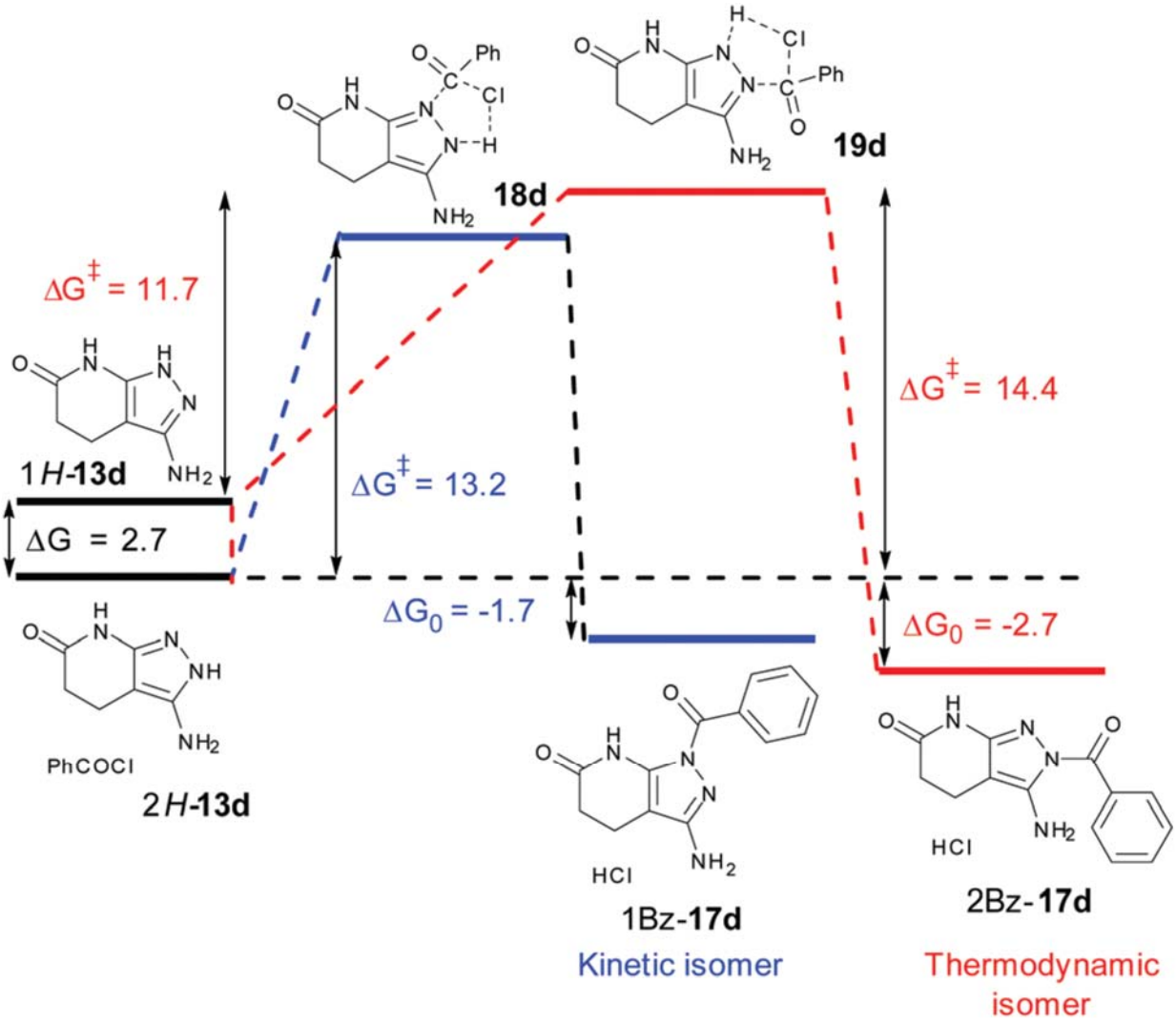
18d
19d
ΔG‡ = 11.7
1H-13d
ΔG = 2.7
ΔG‡ = 13.2
ΔG‡ = 14.4
ΔG0 = -1.7
ΔG0 = -2.7
PhCOCl
2H-13d
HCl
1Bz-17d
Kinetic isomer
HCl
2Bz-17d
Thermodynamic isomer

SCHEME 6

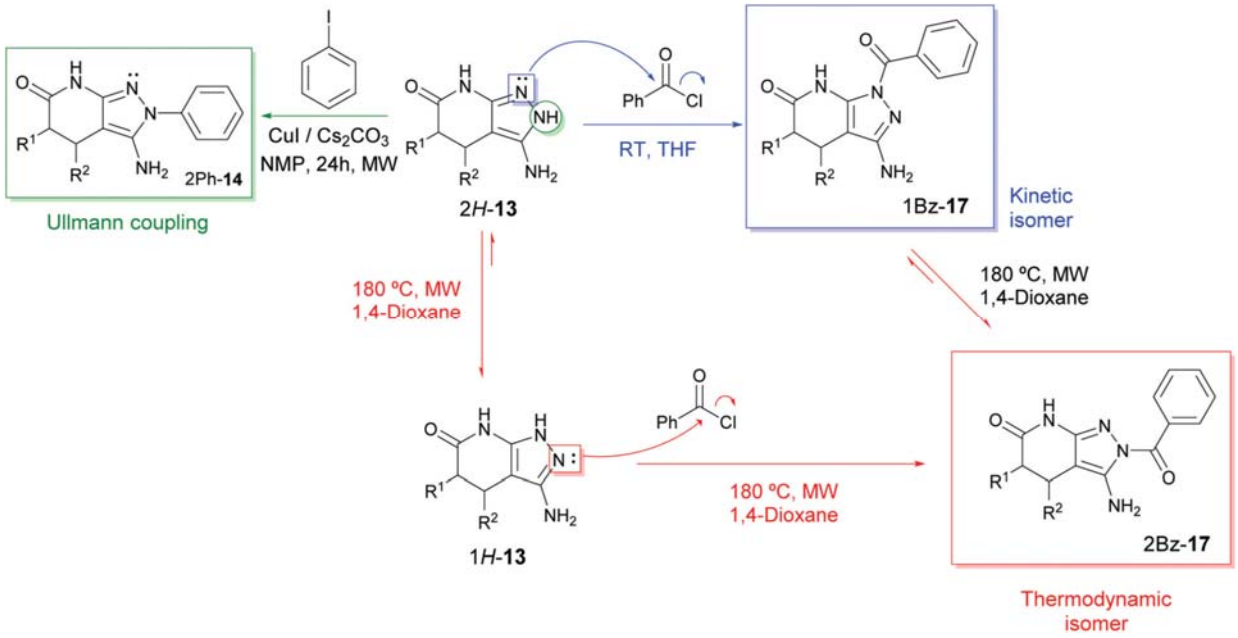
2Ph-14
Ullmann coupling
CuI / Cs2CO3
NMP, 24h, MW
2H-13
RT, THF
1Bz-17
Kinetic
isomer
180 °C, MW
1,4-Dioxane
180 °C, MW
1,4-Dioxane
1H-13
180 °C, MW
1,4-Dioxane
2Bz-17
Thermodynamic
isomer

FIGURE 8

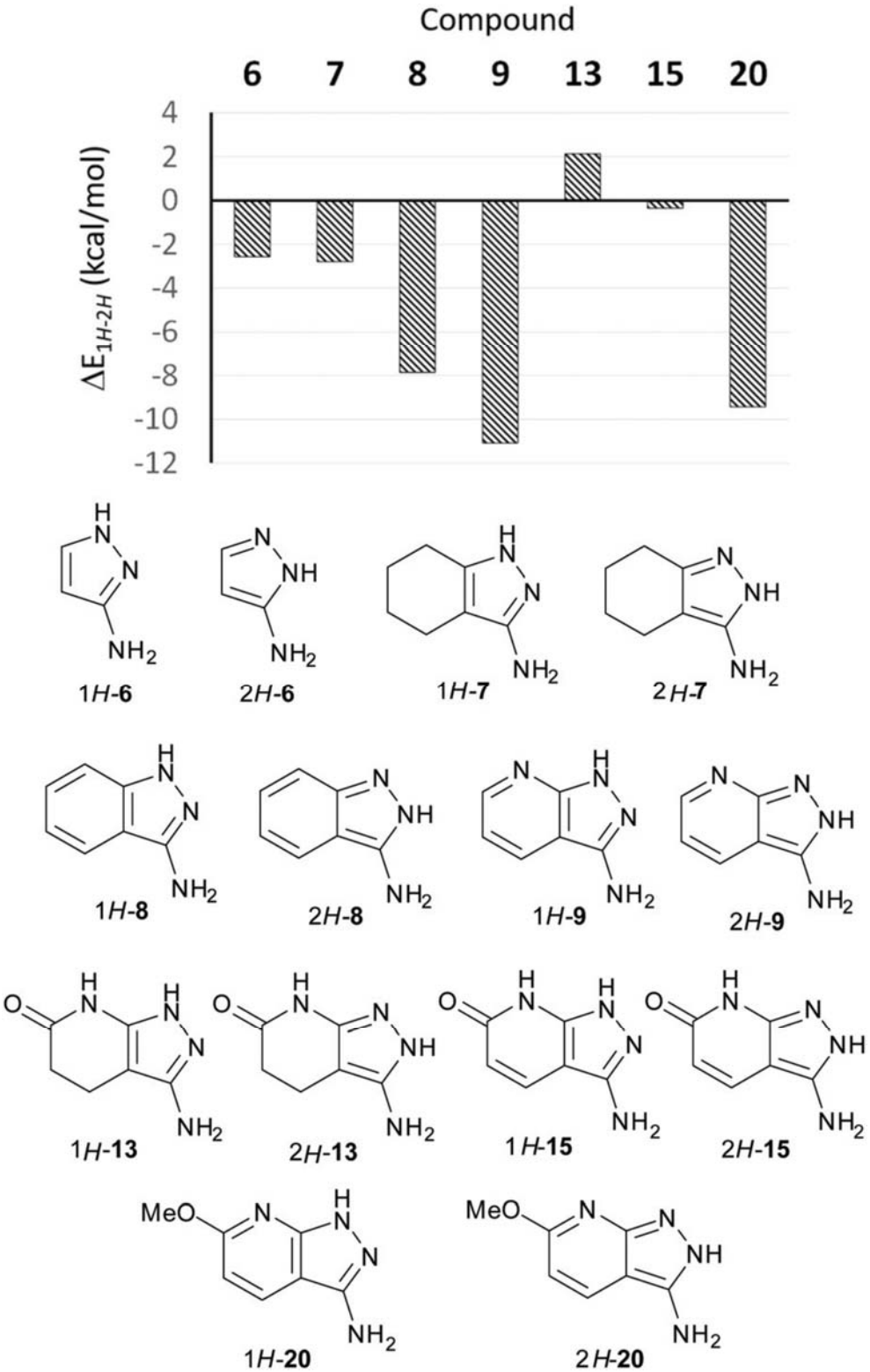
Compound
6
7
8
9
13
15
20
4
2
0
-2
-4
-6
-8
-10
-12
ΔE1H-2H (kcal/mol)
1H-6
2H-6
1H-7
2H-7
1H-8
2H-8
1H-9
2H-9
1H-13
2H-13
1H-15
2H-15
1H-20
2H-20

FIGURE 9

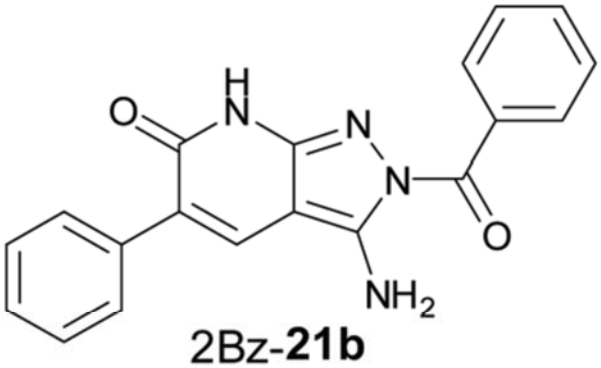

2Bz-**21b**

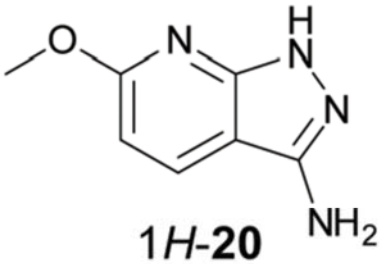

1*H*-**20**

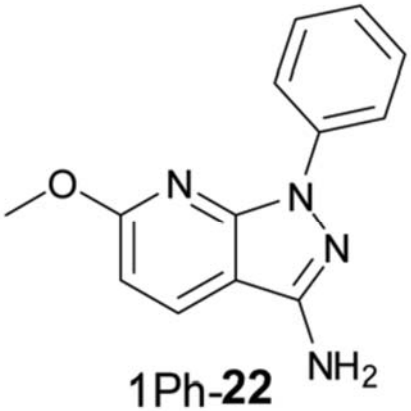

1Ph-**22**

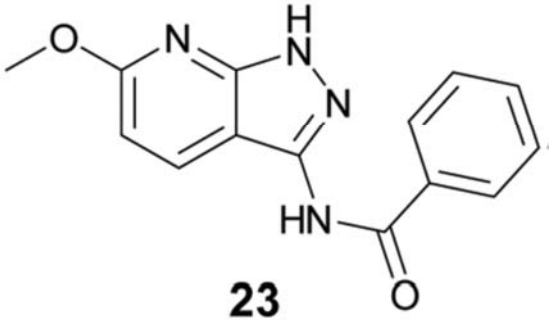

23

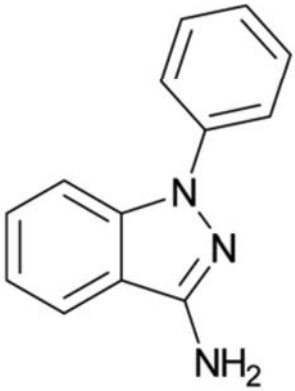

1Ph-**24**

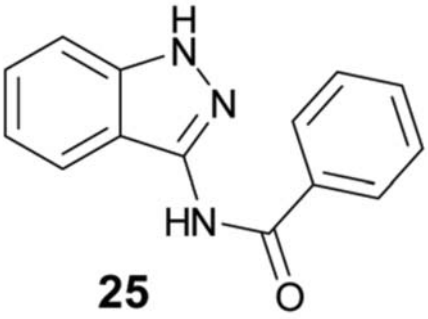

25

FIGURE 10